Volume 1: Cassini Final Report, Rings Discipline Working Group

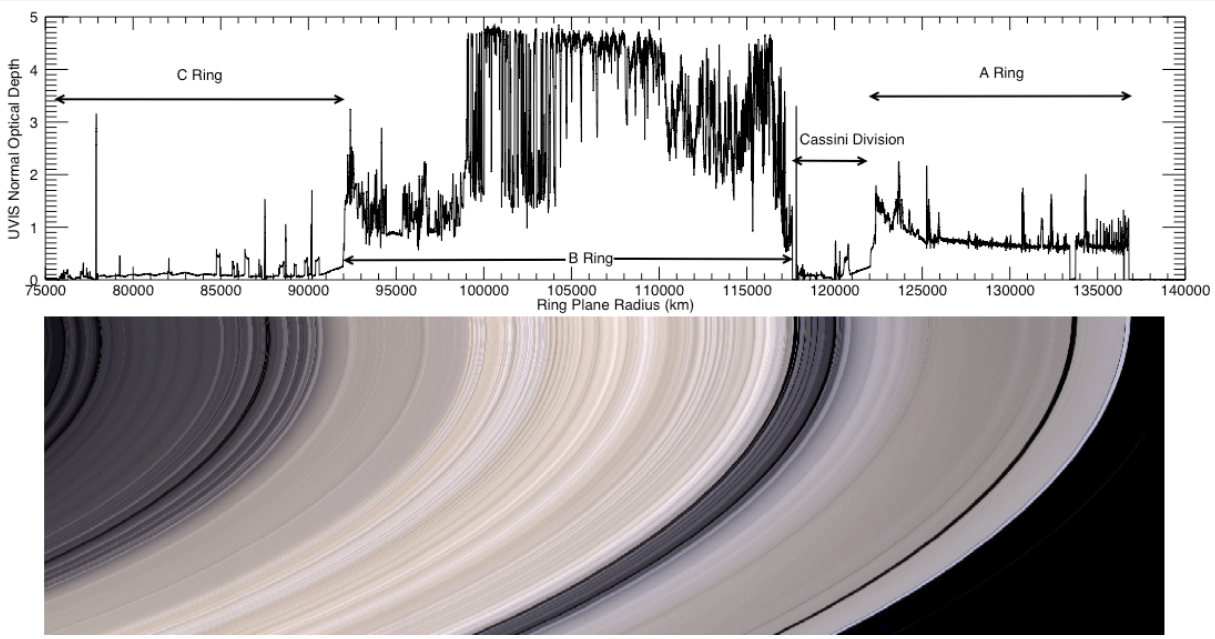

Figure 1: Main rings of Saturn; the image is registered along its top edge with a radial profile of the ring optical depth from a Cassini UVIS stellar occultation. The optical depth (usually denoted τ) is the vertical integral through the ring layer of the particle number density times its cross-sectional area, times extinction efficiency (for the plot above, the efficiency is unity). The B ring – especially its central part – has the highest optical depth, but the highest values shown are just noise limits. Unlabeled regions mentioned in the following text include the series of "plateaus" in the outer C ring, centered on the Maxwell gap near 87500km, which contains an elliptical ringlet. The Encke gap is visible in the outer A ring, around 133600km. The narrow, stranded F Ring is just off the figure at right. Figure from Colwell et al 2009.

RWG Executive Summary:

Cassini has rewritten the textbooks regarding our understanding of Saturn's Rings, a full generation after Voyager first revealed their complex structure. In fact, Cassini studies of Saturn's rings have already been thoroughly reviewed in two sets of review chapters and articles; In the first major review volume "Saturn after Cassini-Huygens", very thorough reviews are given by Colwell et al 2009, Charnoz et al 2009, Cuzzi et al 2009, Horanyi et al 2009, and Schmidt et al 2009, which remain largely valid as of this writing even if they predate many important results. A short, nonspecialist review is given by Cuzzi et al (2010). More recent, complete reviews can be found in the Cambridge "Planetary Rings" book, including Cassini's results prior to the Ring-Grazing and Grand Finale orbits (Charnoz et al 2018, Cuzzi et al 2018, Estrada et al 2018, Hedman et al 2018, Murray and French 2018, Nicholson et al 2018, Spahn et al 2018, and Spilker et al 2018). Finally, all the instrument-based chapters in this volume update the story to the very end of the mission, including results from Cassini's last moments, and some provide exhaustive bibliographies as well. We will attempt to cover the highlights of ring science from beginning to end of the mission as organized by our own goals and objectives, and, in a readable way, provide a thread of continuity connecting Cassini's vast accomplishments to

the big picture of ring origin and evolution. In summary - the rings are changing before our eyes dynamically, and they are much younger than the solar system compositionally.

Waves and collective dynamics: Spiral density and bending waves were discovered by Voyager. They are driven at orbital resonances with various satellites, blanket the A ring, and are sprinkled throughout the B and C Rings. Improved analysis tools have allowed even the weakest of these features to be studied in detail, and they provide powerful constraints on the underlying, local surface mass density on several-km spatial scales. About a dozen spiral density and bending waves in the C ring have been shown to be caused by gravitational and pressure modes inside the planet, potentially constraining the interior structure of Saturn and its rotation rate.

Ring microstructure on sub-km scales is seen everywhere by stellar and radio occultations, and varies on short timescales. Ubiquitous transient gravitational instabilities called self-gravity wakes arise, and are torn apart by differential rotation. These wakes vary in configuration across the rings, and their properties imply a ring vertical thickness of tens of meters or less. An unrelated, axisymmetric kind of microstructure, due more to viscous forces than self-gravity, can also be seen at various places in the denser parts of the rings. Images taken from close orbits, with sub-km resolution, show that fine-scale structure is widespread in optically thick regions, some of it granular and some axisymmetric or streaky. Dense clumps called “straw”, each the size of a convoy of aircraft carriers, are seen in between the dense crests of strong spiral density waves, probably compacted as particles pass through the crests, and subsequently broken apart by collisions.

Embedded moonlets: Analysis of Cassini images have now shown that skirted, embedded 10-km size moonlets are responsible for opening both the Encke and Keeler gaps in the A Ring (see also chapter by the Icy Satellites Working Group). In general, the small ringmoons lying within and near to the rings have very low densities and are likely rubble piles with dense cores. However, moonlets have *not* been found in similar gaps in the Cassini Division or C ring with the ~1 km sizes previously thought necessary to clear them.

Flocks of smaller “propeller” objects of 100-200m size, detectable only in their disturbance of nearby ring material, occupy three radial bands in the A Ring. A dozen or so of the largest of these objects, 0.1-1km in size, wander in semimajor axis, perhaps because of gravitational scattering by the clumpy ring material they interact with. Discrete km-size objects have also been inferred from disturbances at the outer edges of the A and B rings and in the Huygens ringlet of the Cassini Division. One such object has been imaged in the B ring. Some of these objects seem to disaggregate and perhaps reaggregate in place, on timescales of months or years, suggesting ongoing recycling of material driven by satellite forcing, self-gravity, and collisions.

Rings in 3D: Cassini discovered dramatic vertical distortions of the rings, in addition to the well-known spiral bending waves, near Equinox when the sun's illumination was at a grazing angle. The edges of the Keeler gap are noticeably warped, consistent with the small inclination of its central ringmoon Daphnis, but those of the Encke gap are not. The outer edge of the B ring showed alpen-like, spiky peaks and shadows. The outer edge of the A Ring showed a very clumpy structure, lacking distinct peaks but with shadows suggesting vertical relief.

Ring Particle properties: Voyager showed that the main ring particle size distributions tend towards powerlaws ranging between cm-m radii. Cassini has shown that the slope and the

minimum and maximum sizes of these powerlaws vary across the rings. Enhanced collisions in spiral density waves create blizzards of small particles, which seem to affect the brightness and color of the surrounding region. As shown by comparison of occultations at UV, near IR, mid-IR, and radio wavelengths, and by the ring spectra and color, this effect is especially significant in the outermost A Ring, the region most strongly stirred by spiral density waves.

A combination of 10-400 μm thermal emission and scattering, and 2.2 cm radiometry, suggests that ring particles probably have a low density mantle – *ie*, are porous aggregates - but may also have more dense cores. The rings' thermal emission suggests a regolith of nearly pure water ice grains of 10-100 μm size. Cassini 2.2cm radiometry detects a fraction of a percent of non-icy material through the A and B rings, greatly improving on pre-Cassini microwave observations which could constrain the total non-icy material only to less than a few percent relative abundance. However (when combined with spiral density wave surface densities/opacities), 2.2cm radiometry has also revealed what looks like a buried silicate-rich rubble belt in the mid C Ring – possibly the remains of the core of the ring parent.

VIMS spectra show that A and B ring composition is nearly pure water ice without any other identifiable ices such as CO, CO_2, NH_3, CH_4, but there is a strong UV absorption making the rings unusually reddish, that varies in strength from place to place. The red color of the rings is strongest where the water ice absorption bands are deepest, suggesting that the red material resides within the icy regolith grains, and increases radially inwards at a steady rate. A third, more “neutral” non-icy material has a completely different radial distribution. The very low mass fraction of nonicy material (except perhaps in the C Ring rubble belt) provides our strongest constraint on the age and origin of the Rings, as discussed below. The rings’ red color in the UV-visible region may be explained by fragments of carbon-bearing tholins (perhaps similar to material blanketing the surface of comet CG as observed by Rosetta), or (some argue) by tiny iron-rich particles, embedded in the dominant water ice. Recent Cassini *in-situ* results and remote sensing analyses, and HST-STIS observations, favor the organics.

New *in situ* data from CDA and INMS on the Ring-Grazing (henceforth RG) and Grand Finale (henceforth GF) orbits have greatly enriched the ring composition story. Abundant, Fe-poor silicates and organic molecules are associated with the innermost D and perhaps C Rings. Evidence for organics is also found *outside* the rings by INMS. Reconciliation of these *in situ* results with remote sensing is only beginning.

Ring variability with time: The outer edges of the dense A and B rings vary in complex ways with both longitude and time, indicating the interference of multiple free or “normal” modes – possibly the result of large-scale, nonaxisymmetric viscous overstabilities -- with the expected satellite-driven forced modes. The outer 100 km of the B ring shows complex, fine-scale brightness variations possibly caused by these deformations. Gravitational effects of the modes might even play a role in sculpting the narrower gaps in the Cassini Division, so far found to be free of small moonlets.

Channels open and close in Saturn's F ring strands, in response to close approaches by Prometheus, and these effects vary as the orbits of Prometheus and the F ring mutually precess, leading to stronger and weaker gravitational interactions. Kinks and “mini-jets” come and go in the F ring core, excited by small unseen objects at low relative velocities, and more dramatic jets of material lasting months are triggered by objects eccentric enough to crash through the ring at high relative velocities. These violent collisions continue because the entire F ring region

is dynamically chaotic, mostly because of Prometheus, and for this reason the long-term stability of the F Ring core has been problematic. The F Ring has a narrow ``true core'' of large particles, as characterized best by RSS, confined and stabilized by a new kind of dynamical trapping due only to Prometheus. The fine dust seen in images and stellar occultations is a tiny fraction of the F Ring total mass. Clump activity has varied dramatically between Voyager and Cassini.

Vertical ripples or warps covering the inner part of the rings, which have changed even over the duration of the mission, suggest that Saturn's D and inner C rings were tipped relative to its equator several times over the last millennium, and as recently as a few decades ago. Impacts by rubble streams produced by disrupted objects are the most likely cause. Several impacts by individual m-size projectiles have actually been seen and catalogued.

Diffuse rings dominated by tiny dust grains are affected by sunlight and magnetic fields: The source of the E Ring particles has been confirmed as the south polar jets of Enceladus (see section on Icy Satellites, this volume). Several new arcs and ringlets are associated with erosion of small embedded moons. The E Ring and other diffuse rings and ringlets (such as those in the Encke gap) are affected by sunlight and electromagnetic forces as well as by gravity, and thus show seasonal variations in their structure. Some diffuse rings, notably the D Ring and the faint material between the A and F Rings, are modulated by azimuthal variations in Saturn's magnetic field.

The duration and behavior of the “spokes” Voyager discovered in the B ring have been further constrained, though their ultimate cause or trigger remains unknown. Cassini found that they seasonally appear and disappear, probably due to variable photocharging of the main ring layer, and their temporal periodicities match best that of the northern hemisphere Saturn Kilometric Radiation (SKR) during the 2008/2009 timeframe, though contributions from the southern SKR source could not be ruled out. Any association with the Saturn Electrostatic Discharges (SEDs) was ruled out.

Ring mass: Voyager-era estimates of the ring mass were roughly 0.7-0.8 Mimas masses. It was since suggested that the breakdown of the ring layer into opaque clumps (the self-gravity wakes), separated by nearly empty gaps, could allow a lot of mass to be “hidden” in the clumps. Modeling of dozens of spiral density and bending waves over Cassini’s first decade had constrained the mass of the A, C, and inner B rings, so any hidden mass had to reside in the densest parts of the B ring. In the Grand Finale Orbits, the Cassini RSS team tracked the spacecraft to constrain the ring mass by its perturbation on Cassini's orbit, and concluded that the ring mass is not very different from, and likely lower than, our Voyager-era expectations.

Origin and Age of the Rings: The strongest constraint on ring age is provided by the gradual darkening and restructuring of the rings with time by infalling meteoroids. Inferring the actual ring age requires knowledge of the current mass fraction in nonicy “pollutant”, as well as both the incoming meteoroid mass flux and the total mass of the rings. The Cassini Dust Analyzer experiment has determined, cumulatively over the entire mission, the infalling meteoroid mass flux and dynamical population. The mass flux far from the planet is not too different from pre-Cassini estimates. However, the dynamical population is like that of Kuiper Belt objects, so has a lower encounter velocity and is more strongly focussed by Saturn's gravity than thought previously. This means that the flux of meteoritic material actually hitting the rings is probably even larger than previously thought. Combining the ring mass with the CDA-

determined meteoroid mass flux, and estimates of nonicy "pollution" currently in the rings, leads to a ring exposure age of 100-200Myr, perhaps even a little younger than Voyager-era "young-ring" scenarios.

The associated puzzles of "Why is Saturn the only giant planet with rings?" and "Is the ring system young?" have been, if not yet explained, at least illuminated by an emerging hypothesis involving a closely-coupled tidal evolution of the mid-sized icy moons leading to a Saturn-specific dynamical instability of the inner satellite system, with possible disruptions and reaccretion, on the order of 100Myr ago. Constraints from satellite surface geology will need to be folded in to evaluate the plausibility of the scenario.

(1) Overall Assessment of Ring and Dust Science

Not only were all key science objectives listed in the AO and Solstice Traceability matrix successfully accomplished over the course of the Cassini mission, but a number of new science objectives were formulated and addressed along the way, either in response to unexpected results or capitalizing on observational opportunities (both some not originally envisioned, and some in greater numbers than envisioned). When the mission was approved, the AO Objectives reflected a 4-year baseline tour with only 59 orbits, allowing at most 16 Radio occultations, and of course did not incorporate the Ring Grazing (henceforth RG) or Grand Finale (henceforth GF) observing geometries. By the end of the mission, even the four-year baseline tour had been optimized to include 74 (generally shorter) orbits, wasting less time far from the planet, and had also been extended by nine years, tripling the total time baseline for observations relative to the AO. The final tour lasted 13 years, sampling three different seasons and reaching Northern Summer Solstice (the maximum opening angle of the rings as seen from Earth and the sun) which allowed the radio occultations to better penetrate the optically thickest parts of the B Ring. The mission included 282 orbits capturing many new combinations of illumination and viewing angles – important for imaging, VIMS and UVIS spectral reflectance mapping, and CIRS thermal mapping. Datasets returned included 135 ring radio occultations (each at 3 wavelengths), 170,000 ring images (many at < 1km/pxl), over 200 UV stellar occultations, 170 near-IR stellar occultations, 30 solar occultations, and even a few occultations at thermal, mid-IR wavelengths. The stellar occultations made use of dozens of stars with different elevation angle relative to the rings; low-optical depth rings are best studied by low-elevation stars, and high optical depth rings by high-elevation stars. In addition, several complete 2.2cm microwave emission maps or radial scan combinations were obtained in different geometries and resolutions, and 3 active radar backscattering scans were obtained in the RG and GF orbits when the spacecraft was close enough to overcome the fourth-power dependence of radar sensitivity on distance. Moreover, the RG and GF orbits provided In-situ ring particle composition sampling opportunities for CDA, INMS, and MIMI that were not part of the AO plan, and enabled direct determination of the ring mass from spacecraft tracking of the RSS signal. VIMS stellar occultations were not even envisioned in the AO, but were added after selection of the instruments. This new stellar occultation capability provided a very useful wavelength difference compared to UVIS, and an entirely different angular distribution of sources on the sky. Using the Radar as a passive, pencil-beam microwave ring brightness mapper, or to obtain active radar backscattering radial profiles from the rings, were also not part of the original plan.

The overall science data volume return of Cassini was more than 100 times that of Voyager in the instruments they both carried, not to mention the roughly 200 times longer time baseline at interesting resolution, and the numerous unique new remote and in-situ observations provided by Cassini. There is no question that the science return of Cassini vastly exceeded the expectations as described in the AO.

(2) Summary of Key Open Questions

Overall, Cassini has answered many of the questions raised by Voyager, raised new ones, and leaves us with a largely untapped reservoir of data with which to answer them all. These and others are discussed in more detail in section 6.

The overall ring mass is known now, but with low precision and no radial resolution. Is the B ring mass uniformly distributed according to optical depth, or is it even more strongly concentrated in the still nearly opaque central regions? Does the C Ring contain a rocky rubble belt? Future missions with tracking capability and multiple close passes will be needed, and should be planned to also provide a better understanding of why Saturn's own interior is so different from Jupiter's.

Most ring structure is still a puzzle! The irregular structure blanketing the entire B Ring, with lengthscales narrowly concentrated near 80 km in the inner B Ring but covering a wider range of scales from the resolution limit to several hundred km in the mid-and outer B Ring, remains a mystery. In the inner-mid B Ring there are very sharp optical-depth jumps (but not to empty space) that are barely explored and remain unexplained.

The entire ensemble of so-called "plateaus" in the outer C Ring, symmetrically placed around the Maxwell gap in the C Ring (which is known to be caused by structure in Saturn's interior) and incorporating some other empty gaps, Is not understood. The plateaus also contain a unique kind of "streaky" microstructure not seen elsewhere, that was only seen in a limited way during the final orbits.

There are several significant features (A ring inner edge, C Ring plateaus) which have sharp, well-defined boundaries that are defined only by changes in the particle size distribution, across which the surface mass density does not change. This structural control of particle size distribution, or vice versa, is not understood.

The mere presence of the Cassini Division is an unsolved problem, although it is plausible that a strong density wave driven by the 2:1 resonance with Mimas had a role in creating it when the rings were more massive and material filled the region. The apparent lack of moonlets capable of clearing the 13 gaps in the Cassini Division and C ring, especially the 5-6 that have no embedded ringlets[1], is a puzzle. A clue may be found in the apparently non-random spacings of the edges of the Cassini Division bands and gaps, perhaps somehow manifesting gravitational influence of the B Ring outer edge.

The unusually "red" color of the A and B rings, which are more than 95% water ice, seems to be due to organic material, based on a combination of remote and *in situ* measurements. However, composition varies from place to place and on a range of scales.

[1] Cassini Division gaps with ringlets: Huygens, Herschel, Laplace; and without ringlets: Russell, Jeffreys, Kuiper, Bessel, Barnard; C ring gaps with ringlets: G1, Colombo, Maxwell, Bond; and without ringlets: Dawes

Models capable of interpreting color and spectral data quantitatively in terms of underlying composition are inadequate, and need improvement. The hint of a rubble belt of nonicy material buried in the mid-C Ring is intriguing, but remote observations are ambiguous and the analysis of *in situ* observations is only getting underway. Whether or not organics explain the similar, but relatively weak, UV absorption seen in most of the icy moons is not yet known (the dark side of Iapetus has been fit by carbon, nano-iron, and metal oxides). Why is the G Ring parent body, so close to the icy main rings, so dark?

Are the A (and B) ring propeller objects the shards left over from the ring parent? Why do the dozen or so "giant propellers" found only outside of the Encke gap wander in semimajor axis, and what (if any) patterns are present in the evolution? Are there cyclic, self-limiting processes of growth and disruption of sub-km sized objects in the outer A (and B) rings? The F Ring core is stabilized by Prometheus, but what causes its uniformly precessing eccentricity? Do relatively large objects form in regions compressed by Prometheus and go on to crash through the core, creating clumps and strands?

The rings seem to be much younger than the Solar System, based on nominal results to date, and there is one encouraging hypothesis (a 200Myr-ago system-wide instability) providing the proper context, but questions remain including consistency (or lack of it) of the observed icy moon cratering distributions with reaccretion of most of the inner icy moons on that same timescale.

(3) Key Objectives of the Rings Working Group

The original ring objectives from the AO, and those added for the extended Cassini Solstice Mission, are given below. As can be seen in the Table, We assess Cassini as fully successful at least, in all regards. *It cannot be emphasized enough that in almost all cases, there has been far more data obtained, reduced, and archived than the teams have had time to analyze and interpret.*

RWG Science Assessment, matrix format

RWG Science Objectives	AO and TM Science Objectives	RWG Science Assessment	Comments if yellow (partially fulfilled)
Ring Structure and Dynamics	R_AO1		
Ring Particle Composition and Size	R_AO2		
Ring-Satellite Interactions	R_AO3		
Dust and Meteoroid Distribution	R_AO4		
Ring-Magnetosphere-Ionosphere Interaction	R_AO5		
Changing Rings	RC1a		
Ring Temporal Variability	RC1b		
F Ring	RC2a		
Ring Age and Origin	RN1a		
Ring Composition	RN1b		
Ring Structure	RN1c		
Ring Microstructure	RN2a		
New Ring Structures	RN2b		

These objectives are discussed below in more detail.

(4) RWG Science Results

4.1 Prime Mission (AO) Original Objectives (Highest, top-level results)

4.1.1 Ring Structure and Dynamics (R_AO1) - Study configuration of the rings and dynamical processes (gravitational, viscous, erosional, and electromagnetic) responsible for ring structure.

This objective – perhaps the broadest and deepest - was satisfied beyond our initial expectations. Stellar and radio occultations are the most powerful tool for exploring structure at high resolution. During initial planning sessions, the UVIS team was considering dozens of stellar occultations as an optimistic goal, and ended up with over 200, including the novel "turnaround" occultations in which the line of sight to the star moves parallel to the particle orbits, at very low velocity, allowing azimuthal structure to be determined at high resolution in perhaps a dozen radii and structure on the scale of a ring thickness to be addressed statistically. Moreover, VIMS developed a stellar occultation capability of their own that was not part of the original plan, and went on to produce almost 200 occultations of their own in geometries that were independent of and complementary to those available to UVIS, because they observed a different set of stars. All these stellar occultations reside on the Rings PDS node in 1 and 10km resolution format. In addition, RSS conducted 135 occultations at three radio wavelengths (0.94, 3.6, and 13 cm), which all reside on the Rings PDS node in 1 and 10km resolution format, and for which further processing (by diffraction correction) can generally provide 100m or even better radial resolution. More analysis of these data will provide additional surprises and constraints. Review chapters by Colwell et al (2009) and Cuzzi et al (2018) cover the major advances regarding observed ring structure; Schmidt et al (2009) review advances in the theory of dense ring structure, and Horanyi et al (2009) review advances in the theory of electromagnetic influences (most significant on tiny dust grains).

(a) Configuration of the rings: The ``Grand Structure of the rings" **(Figure 1)** was elucidated for the first time by Voyager (reviewed by Orton et al 2009 and Colwell et al 2009). In this section we will discuss the so-called "Main rings" – the A, B, and C ring and the Cassini Division, all of which have optical depth greater than about 0.1 **(Figure 1)**. The A ring is the best understood by Voyager-era theory - blanketed by spiral density and bending waves from nearby moons, with embedded moonlets that carve empty gaps by the process of gravitational shepherding, and a ubiquitous nonaxisymmetric "microstructure" having scales comparable to the ring thickness due to local gravitational instabilities. All of these structural properties have been closely observed by Cassini, in greater numbers, with greater radial coverage, in more geometries, in finer detail, and at better sensitivity than ever before. The B and C rings contain a few of these well-understood features too, but are overwhelmingly dominated by structure on all scales that is simply not understood at present (see subsection e, below). The so-called "Diffuse" D, E, and G rings, and dusty rings associated with various moonlets, have optical depths much less than unity and are a separate class of structure discussed in section 4.1.4-4.1.5. The narrow, kinky F Ring lying just outside the A Ring has captured a niche of its own and is discussed mostly in section 4.2.3.

The local "ring thickness" was a perennial topic of discussion before Voyager, and measurements of kilometers were reported (now known to be better explained by vertical corrugations and/or the inclined F Ring). The single Voyager stellar and Radio occultations showed that ring edges were so sharp that the local thickness - at least at edges - could be no more than tens of meters. Cassini's hundreds of stellar and radio occultations have extended this knowledge to nearly all locations except the opaque central B ring (Colwell et al 2006, 2009; Hedman et al 2007; see also Tiscareno et al 2007). This small vertical thickness means that the rings are not the "many particle thick" classical layer envisioned even in the Voyager era, and have a moderate volume density of 0.01-0.1 (Salo and French 2010) or even larger. There are implications of high volume density for ring viscosity (see (c) below). Another indication of volume density (and thus local dynamics) comes from mutual shadowing. Visual brightness observations have long shown a sharp "opposition peak" that was traditionally interpreted in terms of shadowing in a many-particle-thick layer; however dynamical constraints, and the increased recognition of the importance of coherent backscattering in grainy particle regoliths (see Cuzzi et al 2009 for a review) complicate this interpretation (Salo and French 2010). CIRS observations show a much broader phase effect in particle temperatures, however, that is plausibly shadowing-related, unlikely to be contaminated by coherent backscattering, and consistent with nonclassical rings (Altobelli et al 2007, 2009; Reffet et al 2015, Morishima et al 2017). These thermal studies lead to midplane particle volume densities as large as 0.3-0.4 in the B ring. Finally, analysis of 2.2 cm radiometry is best fit by modeling closely packed, cm-m size particles in the near-field scattering regime (Zhang et al 2017b).

There has been a start taken on modeling of imaging observations of the rings over a wide range of geometries, with an emphasis on unraveling opposition effects of different kinds using classical radiative transfer models, (Deau et al 2013, 2018; Deau 2015). However, interpreting UV, visual, and near-IR observations using realistic models of closely packed particles with rough, shadowed surfaces, which might provide more insight into radial variations of local particle volume density and thus local dynamics, remains in its infancy (see Porco et al 2008 for the only example).

(b) Gravitational processes (self-gravity wakes, spiral waves, and shepherding torques): Probably the longest-known and most widespread gravitational process leads to the *"self-gravity wakes",* caused by local, transient, incipient gravitational instabilities which are stretched into trailing clumps of scale comparable to the ring thickness (indeed defining the ring thickness) by Keplerian shear, keeping the ring in a constant state of frustrated satellite formation (Orton et al 2009, Schmidt et al 2009, Colwell et al 2009). Imaging observations have characterized the effect in the A ring, using the azimuthal brightness asymmetry known for decades, but finding the particle collisional elasticity to be smaller than thought – indicating either a rough surface or a porous regolith (Porco et al 2008). The effect has also been observed and modeled in the thermal IR (Leyrat et al 2008, Ferrari et al 2009, Morishima et al 2014; see section 4.2 of Flasar et al, this volume, and Spilker et al 2018). A "CAT-scan" technique of characterizing the horizontal and vertical scales of these structures as well as their angle relative to the orbit direction was developed based on stellar occultations from a variety of slant directions. These models of the dense gravitational wakes as optically thick "granola bars" or elliptical cylinders (Colwell et al 2006, 2007; Hedman et al 2007a, Nicholson and Hedman

2010, see Colwell et al 2009 for a review) provide valuable mean values of the orientation, width, height, and separation of dense clumps for use in models of ring brightness. The pitch angle of the wakes, relative to the orbit direction, decreases radially inwards as differential rotation becomes stronger.

Perhaps the most obvious, beautiful, and useful gravitational ring structures are *spiral density and bending waves* at isolated satellite resonances. These striking features share the physics of the arms of spiral galaxies but are tightly wrapped like watchsprings (Shu 1984; Schmidt et al 2009). They propagate away from their driving resonance with a decreasing wavelength – density waves move outwards and bending waves inwards. The wavelength itself is diagnostic of the underlying surface mass density on scales smaller than a wave. Thus, spiral density wave measurements provide our best idea of the radial profile of mass density, in regions where they are found. This property is extremely important, because the almost ubiquitous clumping due to self-gravity waves breaks the rings into a set of opaque regions separated by nearly empty gaps, for which "the optical depth" (see figure 1) is of questionable basic value.

For this reason, Robbins et al (2010) suggested that inferences of ring surface mass density from a combination of observed optical depth and particle size distribution might greatly underestimate the ring mass. This reasoning led to a debate as to whether the ring mass could be much larger than Voyager-era estimates, because most of the B Ring (which contains most of the mass) is unsampled by diagnostic density and bending waves, with implications for ring age (see section 4.2.4). The debate tilted in favor of low mass when Hedman and Nicholson (2016) succeeded in obtaining some B ring density wave measurements despite the noisy background, and has now been definitively resolved in that direction by the RSS total mass measurements based on gravitational tracking (section 4.2.4a). The RSS gravity measurements have little or no radial resolution, but used A and C Ring masses as determined from these waves (Colwell et al 2009, Tiscareno et al 2013) and assumed the remainder of the measured mass to be that of the B ring. They do suggest, though, that the surface mass densities obtained from spiral density waves are insensitive to the suggested clumping difficulty.

One important surprise from measuring surface mass density is that several important structural features, long seen in images and occultations, actually manifest as distinct structures not because they have higher local mass density, as was usually assumed, but because their local particle size distribution changes in a dramatic way, making them more opaque than their surroundings *without* much change in their underlying surface mass density. This happens because the surface-to-mass ratio of a particle, or of a distribution of particles, increases as particle size decreases. The effect is seen at the inner edge of the A ring and all of the C Ring plateaus – sharp optical depth jumps are seen where there Is at most a gradual change in surface mass density (Tiscareno et al 2007, 2013a; Tiscareno and Harris 2018. Baillie et al (2011) and Hedman and Nicholson (2014a) show surface mass densities for the plateaus and background C ring, and Colwell et al. (2018) show drops in effective particle size in the plateaus, consistent with a small change in surface mass density despite a large increase in optical depth. This important phenomenon of locally abrupt changes in the particle size distribution is not currently understood, but is clearly of central importance to understanding the formation of these structures.

Another important clue from density and bending waves is obtained from their (sparse) sampling of the C Ring, showing that the surface mass density radial profile differs from the optical depth profile in a fashion most easily explained if the local particles, whose sizes are well known from RSS occultations, are several times more dense in the central C ring than elsewhere in it – possibly hinting at buried rocks in unusually high abundance, and perhaps to a hidden rocky rubble belt (Zhang et al 2017a; see section 4.1.2 on ring origin). Sampling of the B Ring is even more sparse, but generally points to surface mass densities somewhat lower than previously thought (Hedman and Nicholson 2016, Tiscareno and Harris 2018)

An interdisciplinary bonus was the confirmation of the prediction by Marley et al. (1987, 1989), Marley (1990), and Marley and Porco (1993) that density fluctuations in Saturn's interior produced by planetary scale acoustic oscillations (modes) can drive spiral density and bending waves similar to those driven by an external satellite. A number of unidentified waves had been noted by Rosen et al (1991) in Voyager RSS occultation data. Marley and Porco suggested several specific associations between predicted resonance locations and these "Rosen waves". They also suggested that the strongest predicted (two-lobed, or m=2) planetary interior resonance might be associated with the unexplained Maxwell gap, where there was an unexplained eccentric (m=1) ringlet.

Cassini, along with subsequent improvements in the Saturn interior model, have confirmed Marley and Porco's predictions, putting the study of "ring seismology" on firm ground and finding in the process other features likely due to variations in internal structure not accounted for in the simple 1993 interior model. The great advantage of Cassini data is multiplicity and accuracy of occultation measurements, allowing both the number of spiral arms and the pattern speed of the waves to be determined unambiguously, and thus finer associations to be made with theoretical predictions (Hedman and Nicholson 2013, 2014a, Marley 2014). Initially, some Rosen waves, and newly discovered ones (Baillie et al 2011), were found to have the same value of m, something not predicted by Marley and Porco. However, Fuller et al (2016) showed that allowing a compositionally-stratified layer deep inside Saturn could explain these multiplicities because such a gradual density transition would allow different types of modes to mix inside the planet. Next, a two-armed spiral density wave was discovered within the (m=1) Maxwell gap ringlet (French et al 2016b), validating the association of the gap with the strongest (m=2) mode as predicted by Marley and Porco (1993). Finally, Mankovich et al (2018) have recently shown that slightly changing the interior rotation period of Saturn allows the detailed predictions of Marley and Porco (1993) to be very well matched across 16 sets of waves over a wide range of relative strengths, with the strongest perturbation opening the Maxwell gap. In fact, this excellent agreement provides the best constraint yet on the deep interior rotation period of Saturn – a fundamental property that has been elusive because of the almost complete lack of magnetic field azimuthal asymmetry (Dougherty et al 2018, and the MAPS DWG report, this volume). In addition, a new class of density waves has been found in the B and A rings – waves that are driven by density structures of unknown origin, fixed to the body of Saturn (El-Moutamid et al 2016a,b). Surprisingly, some of these wave features are actually seen to drift radially inwards in the rings, indicating temporal changes in Saturn's interior structure on a decade timescale (Hedman et al 2014a, 2017, 2018b). So, ring properties and physics have led to three new, important insights into the deep interior of Saturn.

See also 4.1.3 for more discussion of interactions between satellites and moonlets with the rings, which are mostly gravitational.

(c) Viscous processes: Because of their innumerable particles in a constant state of gentle collisions, the rings act like a gas or fluid and obey the equations of fluid dynamics, with local pressure and viscosity. They spread radially due to viscosity, an important aspect of their evolution that combines with other angular momentum and mass transport processes like shepherding, wave torques, and "ballistic transport" of meteoroid ejecta. The theory of spiral density waves is mature enough that the rate at which their amplitude damps as they propagate can be used to constrain the local ring viscosity (Schmidt et al 2009, 2016; Colwell et al 2009).

A second kind of so-called "ring microstructure", called a viscous overstability , occurs on scales of the ring vertical thickness and is partly driven by viscosity (Schmidt et al 2009). In this effect, a stable (non-growing) radial oscillation can develop that comprises axisymmetric, alternating ringlets of high and low density, that pulsate on the orbital timescale. These structures are aligned with the orbital direction and were first distinguished by subtle Doppler effects in off-axis scattering during Cassini RSS occultations (Thomson et al 2007) but have also been detected using statistical analysis of stellar occultations (Colwell et al 2009, Hedman et al 2014b). They are widespread across the rings and generally found with the expected lengthscales – comparable to a ring thickness - in regions where the optical depth is moderate to high. Self-gravity plays only a small role in these structures.

Viscous overstabilities can take on non-axisymmetric forms as well. For example, in a densely packed ring, collective behaviors akin to those seen in granular flow can occur, and viscous stress can actually decrease the damping between adjacent orbital motions, effectively by locking particles, and therefore their orbits, together. Where there is also the opportunity for double reflection of spiral density waves, as within a narrow, isolated ring bounded by sharp edges, or a so-called "resonant cavity", they can become amplified (Borderies et al. 1985), generating low-order (m=1, 2, 3, etc) modes. The m=1 and m=2 structure of the narrow, sharp-edged rings of Saturn (the Maxwell ringlet in particular, exhibits an m=2 spiral density wave forced by an m=2 acoustic mode within Saturn (see Section 4.1.1b above) but attains an m=1 overall structure) and Uranus may be explained in this way. However, Cassini discovered large-scale, unforced or "free" modes with m=1, 2 and 3 in the outer portion of the B Ring, in addition to the resonant m=2 mode forced by Mimas at the B ring's edge (Spitale and Porco 2010; section 4.2.2). The large-amplitude m=1 mode, in particular, would damp quickly without both the overstabilizing viscous effects described above and the amplification accompanying multiple reflections within the resonant cavity formed by the B ring outer edge and the mode's own resonant radius some 250 km inwards. The discovery of these unforced modes is the first indication of substantial wave amplification on large scales, in broad rings. These modes may have applications to other celestial disks, such as protoplanetary nebulae (Laughlin et al.1997) and spiral galaxies.

Viscosity and pressure due to ring particle collisions determines the ability of ring particles to move from one face of the rings (say the lit face) to the other (unlit) face, and models have been applied to CIRS thermal observations to address this constraint (Flandes et al 2010, Pilorz et al 2015, Morishima et al 2016). Another manifestation of particle collisions would be to pack surface regoliths to varying degrees, depending on local dynamics. CIRS tried

to measure radial variations in particle thermal inertia (higher for more packed particle surfaces), but the complexities of the models, the complications due to small and/or rapidly rotating particles, and the incompleteness of the observing phase space has so far precluded more than a basic determination that the ring particles look like other frosty outer solar system objects. The chapter by Flasar et al in this volume describes how models of ring thermal observations can address these and other issues, in more detail.

(d) Erosional processes: "Pollution" of the mostly icy ring material by meteoroid bombardment, erosion of ring particles into impact ejecta, and restructuring of the rings by "Ballistic Transport" of the ejecta, were first suggested and discussed in the pre-Cassini era (see Durisen et al 1989, 1992; Cuzzi and Estrada 1998; and section 4.2.4c for more discussion). The process is a little subtle and counterintuitive (see more recent work in Charnoz et al 2009 and Estrada et al 2015). Extrinsic meteoroids hit the rings at tens of km/s, not only depositing their substantial amount of nonicy material but ejecting chips of the target ring particle at 1-100m/s; these chips go off on orbits that re-impact the rings, where they become part of a new ring particle. Exchanges of losses and gains of mass and angular momentum can result in significant radial restructuring of the ring surface mass density over a time short compared to the age of the Solar System (given what we now understand about the meteoroid flux; see section 4.1.4).

Signatures of this process can be found both in ring structure and ring composition. To date, intriguing possible correspondences to observed structure have been seen (amongst them the abrupt inner edges of the A and B rings and the odd linear ramps inward of them, and the 80-km scale "irregular structure" in the inner B and inner A rings), and a good match is provided to the smooth compositional profile that accompanies the abrupt B Ring-C Ring boundary. These independent structural and compositional properties suggest a "young" ring age of a few hundred million years, extending the simpler "pollution" argument relying on deposition of nonicy material alone (sections 4.1.2), but the models have many parameters and face new challenges from new discoveries of several kinds (see section 6).

(e) Electromagnetic and radiative processes: Particles in the space environment tend to attain a maximum charge that is only large enough to affect the dynamics of tiny (at most 10 micron size) grains. An entire branch of ring dynamics has to do with resonances involving forcing of tiny charged grains by the periodically fluctuating planetary magnetic field – so-called "Lorentz Resonances" (Burns et al 1985, Schaffer and Burns 1987, see Horanyi et al 2009 and Hedman et al 2018a for reviews of these and other electrodynamical effects). The most obvious places where these processes will be important is in the diffuse rings, such as the D, E, and G rings, which are known to be most easily delineated by their tiny particles (Hedman et al 2009, 2018a). The E Ring shows the most clear influences, including its preference for a near-monodispersion of particle size at around one micron radius, a radial profile with a local minimum at the location of Enceladus, and 3D variations that correlate with the orientation relative to the Sun (Hedman et al., 2012,Ye et al 2016). It is now known, of course, that the E Ring is the frosty breath of Enceladus, and analyses of ISS images have clarified how it is fed in some detail (Mitchell et al 2015).

A second ring phenomenon widely thought to be connected to electromagnetic forces is the flickering of shadowy "spokes" across the A and B rings, discovered by Voyager (see reviews by Orton et al 2009 and Horanyi et al 2009). Various periodicities in the Voyager spoke occurrence rates, rotation rates at spoke boundaries, and the angular and spectral scattering

properties of spoke regions have implicated electromagnetic effects acting on tiny grains (with sizes most recently shown by D'Aversa et al 2010). The tiny grains are probably released sporadically from ring particle surfaces somehow, perhaps by m-size particle impacts, energy beamed from the planet, or magnetic field/plasma instabilities near the ring (reviewed by Horanyi et al 2009). Earth-based observations also contributed to this understanding (McGhee et al 2005). Surprisingly to most of the Cassini team, spokes were invisible on approach and for the first year or more of the mission, first seen only weakly in late 2005 (Mitchell et al 2006). This observation supported an idea first suggested by Nitter et al (1998) that seasonal changes in photocharging by the Sun were responsible. In this theory, dust is constantly being lofted out of the ring plane by impacts, but when the solar elevation is high, electrons are photosputtered out of the dense main ring layer, causing the main rings to be positively charged while embedded in a vertically extended, negatively charged electron plasma. Grains ejected from the rings become negatively charged in this plasma and are swept immediately back into the rings by the strong vertical electric field. The process is like an electrostatic dust precipitator in an industrial smokestack. The theory predicted that at a certain low elevation angle, the electrostatic precipitation would cease and spokes would reappear (Voyager 1 and 2 flybys were both at a time of low solar elevation), and indeed their disappearance again a year or so after equinox proved this to be the case. During the brief time spokes were abundant (roughly 2009-2011), detailed studies of their morphology (Mitchell et al 2013) showed that the spokes had extended active growth times, both radially and azimuthally, and that their activity level was most likely associated with one of the Saturn Kilometric Radiation (SKR) periods, but maximizes at a different longitude in that system than found by Voyager.

Finally, certain dusty ringlets in various otherwise empty gaps in the rings suggest evidence for electromagnetic or even solar radiative control on their predominantly micron-sized grains. One dusty, eccentric so-called "charming" ringlet in the outermost Cassini Division gap, that was *not* very noticeable during either Voyager encounter, always points its apoapse towards the sun due to radiation pressure (Hedman et al 2010a). Several dusty, clumpy ringlets in the Encke gap have similar properties (Hedman et al 2013c). In general, one would expect that these tiny grains are constantly resupplied by generally unseen strands or clumps of macroscopic particles with comparably low optical depths, but such a belt of more massive particles would *not* be influenced by electromagnetic or radiative forces.

4.1.2 Ring Particle Composition and Size (R_AO2) - Map composition and size distribution of ring material.

As described in more detail in section 4.2.4c, understanding the nonicy mass fraction in the rings is critical, as it provides perhaps the strongest constraint on the age and origin of the rings.

(a) Composition (remote sensing): The goal was to determine the composition of the ring material with the best possible radial resolution across the main rings. Spectral observations at UV, visual, and NIR wavelengths are generally insensitive to ring particle size because the ring particles were known to be much larger than these wavelengths from groundbased and Voyager observations. Known ring structure is on scales on 100-300km, so observations needed to be planned to enable VIMS, UVIS and CIRS – all having much lower resolution than ISS – to resolve these scales. Longer observation times allowing deeper

integrations were possible at greater distances, and high SNR spectra of broad segments of the A, B, and C Rings were also obtained. As time went on, we learned more about the observations and about the rings. For instance, Saturnshine was found to contribute organic-looking spectral features in certain geometries (ring longitudes between 120-240^{o} Solar hour angles as observed from high phase angles, for instance). The VIMS and UVIS calibration pipelines evolved and improved as the mission went on, and data analyzed and published early in the mission might still profit from reanalysis. ISS, while having much higher resolution and typically obtaining 3-5km/pxl in extended color sequences, has very limited spectral resolution. In-depth ISS sequences were planned, but only one lit face observation in all 15 filters was obtained in Prime Mission, which was corrupted, so extensive and redundant followup was planned for the "extended" or Cassini Solstice Mission (CSM), over a range of illumination and viewing geometries (see 4.2.6). Regional and local radial variations in color and spectra were seen by UVIS, ISS, and VIMS, greatly expanding geometrical and wavelength coverage to a depth of data that has yet to be plumbed. However, going from observed reflectivity (or I/F, the ratio of observed intensity to that of a colocated Lambert surface) to quantitative constraints on ring particle composition is a somewhat imperfect modeling step, involving the poorly understood way closely spaced particles with rough, grainy regoliths scatter light (see section 6).

Allowing for most of these complexities, VIMS spectral data has been especially powerful in connecting the abundance and regolith grain size of water ice with the relative abundance of other materials. Early in the mission, Nicholson et al (2008) found, and subsequently Hedman et al (2013) showed in more detail, that the redness of the main rings correlated very well with the water ice band depth, suggesting that the UV absorber was spatially colocated with water ice, most likely as tiny, submicron or smaller size inclusions within the water ice regolith grains (new in situ observations may have even detected these tiny few-nm-size inclusions directly – see section 4.2.4b). Detailed studies of radial variation of color and spectra are reviewed by Cuzzi et al (2009, 2018, and references therein). Regarding the actual nature of the UV absorber, a lively debate has continued for a decade as to whether the rings' redness can be better explained by good old-fashioned rust or other metal oxides, as on Mars, or by large, organic molecules like Polycyclic Aromatic Hydrocarbons (PAHs) that give fruits and vegetables their orange-red color (see Cuzzi et al 2009 for a discussion).

Broadly speaking, the optically thinner C Ring and Cassini division are more "polluted" by some spectrally neutral nonicy material than the A or B rings, making them darker at visual wavelengths and decreasing the strengths of the near-IR water ice bands; this is the natural outcome if the darkening material is deposited from extrinsic meteoroid bombardment (Cuzzi and Estrada 1998; Bradley et al 2018; see Cuzzi et al 2009 for a review). More recent results from CIRS thermal models give the ring particle bolometric albedo – another measurement of their nonicy pollutants; it is interesting that, like inferences from visual wavelength reflectivities, the bolometric albedos are not only lower in the C ring and Cassini division but also vary smoothly across the sharp A and B ring boundaries (Morishima et al 2010), as generally predicted by ballistic transport models.

Cassini's late-orbit in-situ observations find plenty of organic material and some silicates, but no discernible free metal or metal oxides (see section 4.2.4b for details). Moreover, the most recent Cassini and non-Cassini studies using both classical and Monte-Carlo ring radiative transfer models agree that the spectra are more consistent with reddish organics than with

other suggested materials (Ciarniello et al 2018, Cuzzi et al 2018b). However, even the best current regolith scattering models simplify the physics and involve several parameters. Because different flavors of "Hapke-like" regolith scattering models lead to systematic, model-based uncertainties in absolute abundances at the factor-or-several level, or even worse, quantitative inferences about abundances must be treated with caution. For instance, Hedman et al (2013) interpreted fine-scale radial color variations in terms of regolith grain size, but this may have been because of the limitations of their (classical) model, whereas other secondary optical-depth-related effects may as likely be the cause. On the other hand, Cassini's UV spectrometer UVIS observed the strong 170nm water ice absorption edge and how it varies across the rings (Bradley et al 2010, 2013); these analyses provide a sensitive measurement of the regolith grain size, which can remove ambiguities in regolith models at comparable wavelengths and lead to absolute abundances of nonicy material (see section 4.1.2 for more discussion of grain size effects). So, while the compositional debate has clarified regarding overall composition, there is a need for considerably more work regarding radial variation and inference of quantitative abundances of nonicy material (see section 6).

Other new contributors to the ring composition were the CIRS far-IR capability[2] and the Cassini 2.2cm Radar, used in radiometer mode[3]. These observations have considerable historical motivation, as microwave observations were the first to constrain the ring composition as nearly pure water ice particles of cm-m size (see Esposito et al 1984 for a review). The basic observation is that the brightness temperature of the rings drops from the physical temperature in the thermal IR, to a small fraction of it in the microwave (thus requiring a low particle emissivity). CIRS was able to get ring spectra covering the transition spectral range between thermal IR and several hundred micron wavelength, resolving inconsistent Voyager-era observations (Spilker et al 2005, 2018, and Flasar et al this volume), and 2.2cm radiometry was used to create sensitive, high-resolution maps of the very low microwave brightness temperature (Zhang et al 2017a,b). Microwave radiometry is unique because the long wavelengths penetrate to depths of several meters in cold water ice (that has a very low microwave absorption coefficient), thus microwaves sample the *bulk composition* of the ring particles in a way that micron and submicron wavelengths cannot. The Cassini 2.2cm radiometry had sufficiently high resolution to separate the A, B, and C Rings into dozens of radial bins, and greatly improved on groundbased interferometry by setting upper limits of a fraction of a percent on nonicy material in the A and B Rings.

Analysis of the 2.2 cm RADAR radiometry observations also found that the C Ring (with up to 6% nonicy material uniformly mixed) is much "dirtier" than the A and B rings (Zhang et al

[2] It had been hoped that the longest wavelength channel of CIRS – advertised as 0.5mm wavelength but more realistically 1mm, could be used as a radiometer in this way, but complicated calibration problems with the Michelson interferometry technique precluded this even after considerable effort by the team.

[3] Little was proposed or expected along the lines of ring science from RADAR in the AO or early discussions, as the team was exclusively focused on Titan. However, as the mission went on and the antenna beam was carefully calibrated, the very low ring brightness temperature was mapped even in the presence of the 10-times-brighter, huge globe of Saturn looming in the complex sidelobes.

2017a,b). The assumption of uniform mixing may seriously underestimate the C Ring nonicy material abundance though; constraints on surface mass density from a handful of spiral density and bending waves strongly suggest that the particles in the same belt of the central C Ring where unusually high abundances of silicates are found, have an internal density several times higher than water ice – far "heavier" than explained by a mere 6% in uniformly mixed silicate dust. The situation suggests buried solid chunks of nonicy material – silicate or carbonaceous – in large volume fraction. This "rubble belt" is what we might expect the remains of a disrupted core of a differentiated object to look like. However, modeling the microwave emission/scattering problem in the main rings is very difficult, since the particle sizes and separations are not much larger than the wavelength, so approximations are needed even in the very best current models, leading to some degree of compositional uncertainty; moreover these analyses are insensitive to the *nature* of the nonicy material.

Recent comparisons of spectral properties of the main rings with those of the ringmoons and classical icy moons are provided by Filacchione et al (2012, 2013, 2014), and other recent reviews are by Cuzzi et al (2009, 2018a). For complementary discussion of the ring composition based on *in situ* observations (not part of the AO objectives), which are especially relevant to the D Ring, see section 4.2.4. The so-called "diffuse" (D, E, F, G) rings and smaller rubble belts) are discussed in section 4.1.4, both regarding structure and composition.

(b) Size Distribution: Even before Voyager, it was known that by far most of the main ring particles were in the cm-few meters size range, and for this reason microwave wavelengths were expected to be the most powerful at specifying their details. To this end, Cassini's observation planning incorporated 135 radio occultations of the main and F rings, at three wavelengths: 0.94, 3.6, and 13 cm. These occultations provide the direct-path optical depth at all three wavelengths, clearly showing local and regional differences in the abundance of the smaller particles (a few cm in radius). In addition, the off-axis scattering (so-called bistatic scattering) of the radio beam can be used to constrain variations in the particles at the *large-size* end of a (usually) powerlaw size distribution, as well as the slope of the powerlaw (eg Zebker et al 1985; Cuzzi et al 2009). The RSS occultation profiling observations have been reduced, corrected for diffraction, and provided to the Rings Node of the PDS; some examples are shown in Cuzzi et al 2009 (figures 16.1a-16.2). Distinctions as subtle as changes in the slope of the powerlaw size distribution and the minimum and maximum particle size between typically a few mm and a few meters can be discerned. In addition, stellar occultations contribute information on the relative abundance of smaller particles.

Some generalities can be extracted even at this preliminary stage of the investigation. The fraction of small particles increases outwards through the A ring based on the RSS data, consistent with more vigorous collisions associated with the increasing radial density of resonances and spiral density waves (Cuzzi et al 2009; Becker et al 2016, Jerousek et al 2016). In the RSS data, C Ring "plateaus" show local drops in the differential optical depth, characteristic of locally fewer wavelength-size particles, and a similar effect is seen crossing from the outer C Ring to the inner B ring, and from the outer Cassini Division to the inner A Ring – with the optically thicker rings having relatively fewer wavelength-size particles lying near the small end of the size distribution (Cuzzi et al 2009).

Stellar occultation variance data[4] from UVIS provides an independent and complementary particle size determination to the RSS data. All of the C ring plateaus and narrower "embedded ringlets" have a smaller mean particle size compared to the background C ring revealed by UVIS occultation variance data. The background C ring has an undulating optical depth over scales of hundreds of km, and effective particle size correlates with this structure; this may suggest size-dependent dynamical transport within the ring. The innermost 700 km of the B ring, and regions around the strong resonances in the A ring, exhibit different effective particle sizes based on occultation variance (even though self-gravity wakes in these regions dominate the signal). There is a marked decrease in effective particle size coinciding with the Mimas 5:3 bending wave in the outer A ring. This and other observations suggest a vertically extended haze of small particles across the wave; oddly, the effect is not seen in the nearly *density* waves where collisions might be expected to be even more vigorous. The variance in the Cassini Division "ramp" reveals the particle size distribution there to be more similar to the A ring than to the Cassini Division, with a discrete increase in effective particle size at the inner edge of the ramp. On the other hand, the comparable C ring-B ring boundary transition is more gradual in variance and implied particle size (Colwell et al. 2018).

More information on particle sizes can be gained by comparing the local surface mass density, from wavelengths of spiral density and bending waves (see Colwell et al 2009; Schmidt et al 2009) with the local optical depth. For identical particles, the opacity (ratio of optical depth to surface mass density) is inversely proportional to particle size. Based on a number of observations of spiral density waves, there seem to be only very smooth, or no, dramatic changes in surface mass density across the plateaus or across the inner A ring boundary (Tiscareno et al 2013a, Colwell et al 2009; section 4.1.1b). Because the optical depth *does* change abruptly by a factor of several, there must be a corresponding abrupt change in the opacity at these locations, requiring a change in the particle size distribution. The sense of this is that the particles are on average smaller in the plateaus, and in the inner A and B rings, than in adjacent material, consistent with the variance data noted above. But yet, RSS occultations show that these same regions have *fewer* cm-size particles, requiring either that there must also be fewer large particles, or that the largest particles are smaller, in the plateaus and similar regions. All together this suggests narrower size distributions for the plateaus, and inner A and B Rings, than for their surroundings – relatively fewer particles at both size extremes. There is currently no explanation for this strong structural control on particle size, with very abrupt boundaries.

An important kind of "size distribution" is the size distribution of regolith grains on the surfaces of ring particles. While not what a dynamicist would call a "ring particle", these grains, along with their underlying material composition, determine the spectral signature at any wavelength. Regolith grain sizes are usually best determined in and around strong absorption bands. UVIS, for instance, sees the strong water ice "edge" at 170nm, and from the details of its position determines a regolith grain size of about 5 microns (Bradley et al 2010, 2013). However, at longer wavelengths (say, the near-IR water bands), larger grain sizes in the tens of microns

[4] Showalter and Nicholson (1990) introduced this technique to relate the excess variance in the occultation signal (about a radially variable, locally defined mean) to the size of the largest local particles.

are generally derived (Cuzzi et al 2009, Clark et al 2012, Filacchione et al 2012, 2013). This is consistent with the idea that shorter wavelengths sense and are scattered by smaller scale structures. Indeed, even before Cassini, models by Poulet et al (2002, 2003) of Earthbased spectra of the rings covering the 0.3-4.5 um spectral range required very broad regolith size distributions – from 10 microns to several millimeters. Analyses of the long-wavelength rolloff from much longer wavelength CIRS data (Spilker et al 2005), and a 30 micron ice absorption feature (Morishima et al 2012), suggest (not surprisingly) a broad size distribution from tens of microns to centimeters radius, with the larger ones perhaps starting to merge from regolith particles to freely-floating particles. Much more work is needed with improved regolith radiative transfer models and broader spectral ranges.

The so-called "diffuse rings" have their own distinct size distribution – generally dominated by micron-sized particles that diffract, rather than backscatter, light at UV, visual, and NIR wavelengths (see section 4.1.4).

4.1.3 Ring-Satellite Interaction (R_AO3) - Investigate interrelation of rings and satellites, including embedded satellites.

The first actual sighting of a small moon embedded in a clear gap was Pan, in the A Ring Encke gap (Showalter 1991; see Colwell et al 2009 and Orton et al 2009). Cassini quickly found a second example: Daphnis, in the Keeler gap, has an inclined orbit and the wavy edges it imparts to the gap flap vertically (Weiss et al 2009). The known dimensions and masses of these objects (Porco et al 2005, 2007), combined with the estimated ring viscosity, provides our best validation of the "shepherding torque" theory (Goldreich and Tremaine 1980, 1982; Schmidt et al 2009). Cassini then embarked on an extensive, systematic mapping of the other multiple empty gaps in the Cassini Division and C Ring over the duration of the mission, coming up emptyhanded, and (even though not every longitude of every gap was mapped) concluding that these gaps *do not seem to be cleared by moonlets (*Spitale 2017*),* at least based on the shepherding torque theory as currently understood (Schmidt et al 2009). Clues about other gap-clearing processes may be found in some of the details of the edge locations of the Cassini Division gaps (Hedman and Nicholson 2010, Spitale and Porco 2010, French et al 2016a). However, there are no corresponding clues regarding the few C Ring gaps lacking moonlets, which may instead be explained in the context of whatever mystery process generates the C Ring plateau ensemble, with which the unexplained gaps are associated. It's ironic that the Voyager imaging team redirected resources late in the planning phase to test a (then-new) hypothesis for gap-clearing by searching for gap-embedded moonlets, but resource and time constraints forced a choice of targeting only one gap, and as it turns out, the Cassini Division where they looked was not the right place (Smith et al 1982).

Ring edges can also be maintained by single, isolated resonances, as at the outer edges of the B ring (Mimas 2:1 resonance; Spitale and Porco 2010 and references therein) and the A ring outer edge (Janus 7:6 resonance; Porco et al 1984). Recently El Moutamid et al (2016) and Tajeddine et al (2017a) showed in detail how Janus actually is able to create an abrupt edge for the outer A Ring and restrain its spreading, even as it swaps orbits back and forth with Epimetheus, in somewhat of a team effort with all the other ringmoons and resonances acting on different parts of the A ring, so the classical "shepherding" theory seems to be in good shape.

The kinky, stranded F Ring has a more complicated, often chaotic, relationship with its nearby moons, though (see section 4.2.3).

A special kind of embedded moonlet is one that is too small (smaller than 1 km radius) to actually open a gap; these were predicted by Spahn et al (1994), but most Cassini scientists were surprised to actually see some, initially in the SOI images (Tiscareno et al 2006). These have been dubbed "propellers" by virtue of the disturbances they create, which are too weak to prevent viscosity from backfilling the disturbance before the next encounter of the moonlet with the same material. It seems there are on the order of a million of these objects in the A ring, and they are confined mostly to three distinct bands in the A Ring (Sremcevic et al 2007, Tiscareno et al 2008). There have been reports of propellers in the B Ring as well (Sremcevic et al 2012, 2013, 2014a, 2014b). It is not currently understood whether these objects are shards of a ring parent, or are somehow spontaneously forming and perhaps dispersing in place (Esposito et al 2012). The three A ring propeller bands are anticorrelated with the "halos" of large spiral density waves, and correlated with the strength of self-gravity wakes, which might favor the local formation idea or might simply indicate changes in the photometric balance or local viscosity that causes propellers to be visible. A subset of much larger objects, dubbed "Giant Propellers" was discovered, which could be tracked and found to be evolving in semimajor axis (Tiscareno et al 2010). This discovery motivated significant dedicated observing during the extended mission (see section 4.2.8). Meanwhile, the theory of these disturbances has been actively discussed and continues to advance (Schmidt et al 2009, Crida et al. 2010, Pan and Chiang 2010, 2012, Rein and Papaloizou 2010, Pan et al 2012, Bromley and Kenyon 2013, Tiscareno 2013, Seiler et al. 2017).

A possible physical extension of these objects to smaller sizes has been seen in the optically thicker bands of the C Ring (including the plateaus) and Cassini Division (including its outer ramp); so-called "ghosts" or partial clearings appear in UVIS occultations with very small lengthscales (Baillie et al 2013). These are thought to be caused by relatively large ring particles – maybe meters to tens of meters in size – smaller than the A and B ring propellers (objects so small would not clear gaps in the generally higher optical depth, and more strongly stirred, A and B rings). These objects would need to be more than 3 times larger than the largest ring particle in a powerlaw size distribution in order to create the "ghost" clearings.

Fleeting glimpses of what appear to be embedded Keplerian objects have also been obtained near the edges of several rings and ringlets. At the outer edge of the A Ring, the so-called "Peggy" object was seen briefly (Murray et al 2014), seemingly getting ready to break free of the main rings. This exciting moment might, it was thought, allow the object to be spun away from the rings due to ring torques such as modeled by Charnoz et al (2010) – an effect by which the age of the rings might be constrained (see also section 4.2.4c). However, Peggy actually was reabsorbed back into the rings and apparently broke into several pieces, proving that leaving home can be difficult. Moderately large Keplerian objects, but still too small to be seen directly, were also seen near the edges of the A ring's Keeler gap (Tajeddine et al 2017b), in the Huygens ringlet of the Cassini Division (Spitale and Hahn 2016), and near the outer edge of the B Ring itself (Spitale and Porco 2010; see also Cuzzi et al 2018a). It has been suggested that many or even all of these objects are transient, forming by compaction due to satellite perturbations, and then being disrupted as they increasingly stir the regions around them (Esposito et al 2012).

Finally, it cannot be forgotten that all the wonderful dynamical relationships we are starting to understand between the rings and various moons depend on a good understanding of the orbital dynamics of the moons themselves, and the so-called "ringmoons" in particular, that interact strongly with the rings (Spitale et al 2006, Jacobson et al 2008, Tajeddine et al 2013). Additional results can be found in the ISS team report. Of special importance is the paradigm-breaking observational result of Lainey et al (2017) that the midsize icy moons of Saturn, from Mimas through at least Rhea, are tidally evolving outwards much faster than had been previously assumed based on traditional tidal "Q" theory. This was extremely surprising, because Saturn's interior had been thought to be quite non-dissipative, like Jupiter, with a high "Q" value (see Saturn section). A more recent tidal theory suggests that "Q" is highly frequency dependent, and that moons get trapped on a comb of low-Q frequencies that slowly decrease as Saturn's interior structure evolves, driving the entire set of moderate-sized icy moons outward at a more or less distance-independent rate instead of the strongly distance-dependent rate of traditional tidal theory (see, eg, Fuller 2016). This new perspective has profound implications for the origin and (now increasingly believed to be) geologically youthful age of the rings (section 4.2.4c).

4.1.4 Dust and Meteoroid Distribution (R_AO4) - Determine dust and meteoroid distribution both in the vicinity of the rings and in interplanetary space.

(a) The diffuse rings: The so-called "diffuse" rings (D,E,F,and G) are best studied by tracing their micron-size particles. Such small particles scatter UV, visual, and near-IR light into small solid angles in the forward direction so they may be more easily detected than in the lower brightness of their larger particles, which is spread over more angles near backscattering and also may be subject to the low brightness of individual particles. In all these cases where only fine dust belts are observed, it is generally accepted that a larger-particle "skeleton" – or some small parent moonlet - must be present to resupply the micron-sized material, which is rather quickly lost (Burns et al 1984; Hedman et al 2018a). Based partly on observations of charged particle depletions (Van Allen 1982; see also MAPS chapter in this volume for Cassini-based examples), the G ring has long been known to contain an underlying rubble belt or arc of macroscopic particles (see reviews by Orton et al 2009 and Hedman et al 2018), and Cassini discovered that the ultimate source of this rubble belt is a 0.5km size, highly nonspherical object called Aegaeon, which has a very dark, primitive-body type surface (Hedman et al 2011a). Moreover, Aegaeon is trapped in a 7:6 resonance with Mimas (Hedman et al 2007, 2010).

Several other dusty arcs of material were discovered, supplied by the small moonlets Anthe, Pallene, and Methone – of these, Methone and Anthe are trapped in Mimas resonances (Hedman et al 2009b). A composite "dusty ring" phase function and size distribution was obtained from wide phase angle coverage of the D and G rings, for application to so-called "Debris Disks" around young stars (Hedman and Stark 2015); a certain similarity in the two ring phase functions may point to some family and/or process similarity in the particles – such as an aggregate, fractal structure. The D ring shows several kinds of time variability, and is discussed more in section 4.2.2. Also, the giant, diffuse "Phoebe ring" (discovered by Spitzer; Verbiscer et al 2009) was further constrained in extent, dynamics, and particle size using shadow-edge imaging observations (Tamayo et al 2014, 2016).

A disadvantage of necessary reliance on forward scattering for the diffuse rings, is that it is essentially diffraction, and only weakly dependent on composition, so the composition of these rings is not quite as well known. Even when there is some signal in backscattered intensity or reflectivity, it remains problematic to derive even albedos for the large F and G ring particles (whose scattering would be compositionally diagnostic) because their optical depths are variable and/or small, and so uncertain. The F Ring is known to be dominated by crystalline water ice (Vahidinia et al 2011, Hedman et al 2011b) but may be significantly polluted by drifting G ring material (Clark et al 2012, see figure 3.22 of Cuzzi et al 2018a, and section 4.2.3 for more F Ring discussion). By comparison, the composition of the E ring is known very well from CDA *in-situ* sampling (mostly water ice, with embedded organics and salt, all characteristic of the underground Enceladus ocean from which it comes); its structure is discussed in section 4.2.1. In-situ sampling of nanoparticles in the D Ring are discussed below and in 4.1.5 and 4.2.4b.

(b) The extrinsic (interplanetary) mass flux was a primary goal of Cassini. The CDA Instrument paper (Srama et al 2005) estimated detecting 100 extrinsic particles of micron-size and larger, and this is, in the end, just about what they found. However, early in the mission it started to look difficult or impossible to measure it directly (it's a very dusty system in reality), so an indirect approach was explored, looking for dust ejecta haloes around Rhea and Tethys, by analogy to Galileo results at Jupiter (Sremcevic et al 2005); this led to only upper limits and an initial conclusion that the extrinsic meteoroid flux was lower than previously assumed. However, the basic, direct approach, simply counting up the detections and velocities of small particles with identifiably extrinsic orbits, was ultimately successful, partly due to the much longer time baseline of the CSM (13 years) relative to the baseline mission (see below). The lack of indirect detection (satellite dust haloes) was reconciled after the fact by uncertainties in the ejecta yield model. For example, the ongoing "snowfall" caused by Enceladus' geysers might have influenced/changed the mechanical surface properties of Rhea and Tethys compared to the Jovian icy moons. Future analyses of thermal inertias might provide useful constraints on satellite surface properties, in this regard.

The CDA meteoroid mass flux measurement works as follows (Kempf et al 2018; see CDA chapter of this report). For each particle detected entering the instrument there is a instrumental ambiguity that allows two equally valid predetection velocity vectors. A lower limit to the incident mass flux comes from only the 25 particles for which both velocity vectors trace back to extrinsic projectiles, from beyond Saturn. An upper limit of a sort also includes the 75 or so particles for which only one of the velocity vectors requires an extrinsic origin. Because the size distribution of the detected particles is not well known, the largest particles might carry most of the mass, and their rarity suggests that the nominal detection values could be a lower limit. For instance, a solitary 250um particle was not included in the mass flux calculations (including it would increase the mass flux by a factor of five) and another year of mission time might have captured more large particles. Future, more detailed (perhaps Bayesian) analyses might refine the uncertainties more, but at present it seems that the nominal CDA "minimum flux" is conservative. The values for the minimum flux "at infinity" – before gravitational focusing by Saturn – are within a factor of order unity of pre-Cassini assumptions (Cuzzi and Estrada 1998). However, the CDA discovery that the pre-Saturn orbits were dynamically "KBO-like" (low eccentricity and inclination) rather than "comet-like" (and thus have lower encounter

velocities) than previously assumed, leads to an order of magnitude increase in Saturn's gravitational focusing factor and thus in the flux at the rings. The implications of this new result for models of ring structural and compositional evolution, which have multiple parameters (Estrada et al 2015) are not yet well understood but they are unlikely to allow a ring age older than previous estimates of some hundreds of millions of years.

Along the lines of mass flux into the rings, we should mention flux at larger sizes as perhaps providing additional constraints on ring evolution; as yet, no effort has gone into merging these datasets and results. An observation by RPWS only reported at meetings (Gurnett et al 2004) may suggest impacts by dozens of particles during the 30 minutes Cassini was skimming across the face of the rings at SOI; significant theoretical development is needed to translate these observations into responsible projectile sizes (sand-grains?) but if this can be done, the rates would surely be of interest. Impact ejecta trails from a handful of meter-sized particle impacts were imaged by ISS (Tiscareno et al 2013, Schmidt and Tiscareno 2013); UVIS mounted an early attempt to detect actual impact flashes themselves but subsequent thought and modeling concluded that the flash could only be seen in the near-IR (Chambers et al 2008) so the UVIS searches were discontinued. Perhaps a simple, large FOV, NIR photometer experiment to monitor impacts might be considered for a future mission. Finally, as discussed in section 4.2.2, there is evidence for multiple impacts on the rings by 1-10km size objects over decades and centuries.

4.1.5 Ring Magnetosphere-Ionosphere Interactions (R_AO5) – Study interactions between the rings and Saturn's magnetosphere, ionosphere, and atmosphere.

It has long been known that the rings have an "atmosphere" of their own due to photosputtering and meteoroid bombardment, and interact with both the magnetosphere and the planet, even reducing the ionospheric electron density (Shimizu 1982, Connerney and Waite 1984). During Saturn Orbit Insertion (SOI) Cassini obtained the first-ever *in situ* measurement of the ring atmosphere, and it was a big surprise. It had been expected to be dominated by "water products" (WP; molecules and ions of H_2O and its fragments) but instead CAPS found it was dominated by neutral and ionized O and O_2 (Tseng et al 2010). The observations and theory are reviewed in Cuzzi et al 2009; essentially, WP recombine on ring particle surfaces but O and O_2 do not, building up in the ring atmosphere without freezing out or adsorbing onto ring particle surfaces, and ultimately filtering out to the magnetosphere and into the planet (Tseng et al 2010). Since that review, the effect has been modeled in more detail, and the observed seasonal variation of magnetospheric oxygen ions transported from the rings (see MAPS DWG report) suggests that photosputtering of ring ices dominates over material from Enceladus in producing the ring atmosphere (Tseng et al 2010, 2013; Elrod et al 2014). This discovery of the ring atmosphere alone would satisfy the AO objective, but indeed during the RG and GF orbits, Cassini discovered far more about the particulate component of the ring "atmosphere" and its flux into the planet – the so-called "ring rain" long speculated upon (eg, Connerney and Waite 1984). We discuss this in detail in section 4.2.4.

The diffuse E and G Rings interact in more intimate ways with the magnetosphere; their tiny grains get charged and undergo electromagnetic forces (section 4.1.1e).

4.2 Extended Mission (CSM) Objectives:

The objectives below were developed in 2010, to prioritize upcoming planning by focussing on specific problems, either unresolved AO goals or unexpected new phenomena, and to take advantage of the unique geometries of the Cassini Solstice Mission (CSM).

4.2.1 Changing Rings (RC1a) – Determine the seasonal variation of key ring properties and the microscale properties of ring structure, by observing at the seasonally maximum opening angle of the rings near Solstice.

The emphasis here is on "observing at the seasonally maximum opening angle of the rings near Solstice". The dominant operative intention was to take advantage of the maximum ring opening angle as seen from the sun and Earth, to (a) allow CIRS to determine the energetics of thermal heating and cooling of the rings as they opened to their maximum opening angle to the sun, and (b) allow RSS occultations to penetrate the most opaque parts of the rings – the central B ring – which they had not yet been able to do even during the maximum opening angle allowed during Prime Mission (21^{o}). The difference relative to true maximum opening angle of 23.7^{o} can be critical for RSS, as it appears in the exponential of the optical depth term. The objective was very well satisfied, in that 36 more radio occultations were obtained, with various combinations of resolution and sensitivity, at opening angles larger than available during prime mission and more suitable for probing the dense B RIng. The data have been reduced and deposited in the Rings PDS node at 1 and 10km spatial resolution. CIRS also obtained data over a wide range of opening angles; one important conclusion has to do with the seasonal cooling of the rings through equinox; their minimum temperature is considerably larger than instantaneous thermal equilibrium with Saturn's reflected and emitted energy, constraining the internal density of the particles (at least in the A ring where the model was applied) to be closer to solid ice in the central A ring than in its inner or outer regions (Morishima et al 2016). Perhaps this can be correlated with the radial variation of self-gravity wakes and/or the radial distribution of "propeller objects".

When this goal was written, it was still not known as to whether the spokes would vanish again, and if so, exactly when and under what geometrical conditions. Indeed that situation is now well understood in terms of photocharging of the main rings (section 4.1.1e).

The diffuse E Ring, composed largely of micron-sized grains jetted out of Enceladus, deforms and changes shape with the seasons in response to the elevation angle of the sun, as solar radiation pressure influences the orbits of these tiny grains (Hedman et al 2012).

The waxing and waning of the magnetospheric oxygen ion content is dominantly seasonal – implicating photosputtering of ice in the main rings rather than impacts by grains from Enceladus, one previous candidate (Tseng et al 2013).

4.2.2: Ring Temporal Variability (RC1b)- Determine the temporal variability of ring structure on all timescales up to decadal for regions including Encke gap, D Ring, F Ring, and ring edges by substantially increasing the cadence and time baseline of observations.

The rings are changing before our eyes. The F Ring may be the most extreme example of time variability, and merited its own strategic objective (section 4.2.3). Here we discuss other aspects of ring temporal variability.

The sharp edges of the A and B Rings flop around loosely, revealing the fluid nature of the rings. The A ring outer edge seven-lobed structure derives from a 7:6 resonance with

(mostly) Janus, and it reorganizes itself, diminishing in amplitude, when Janus swaps to its outer orbit and the resonance moves off of the A Ring edge (Spitale and Porco 2009, El Moutamid et al 2016c). The B Ring outer edge is more complicated, showing the predicted two-lobed forcing of the Mimas 2:1 resonance, but in addition, showing interference with m=1, 2, and 3 patterns that are probably free modes driven by ring pressure and viscosity. Sometimes the pattern almost vanishes because of this interference (French et al 2010, Hedman et al 2010, Esposito et al 2012, Nicholson et al 2014, Spitale and Porco 2010; see section 4.1.1c)

Saturn's innermost ring – the D Ring – is only visible with effort and in favorable geometry. However, after the F Ring's fireworks, it has provided some of the most interesting evidence for time variations (usually observed by virtue of its fine dust component, in forward scattering geometries, as discussed in section 4.1.4a). Hedman et al (2007b) first noticed that its structure of irregularly spaced bands or belts had changed dramatically since Voyager. They also pointed out a pattern that they interpreted as a vertical spiral ripple, and suggested that the ripple was the result of an ongoing wrapping up by differential node regression of a tilted mean ring plane. From the wavelength of the wrap, which shortens with time, they dated the event to the early 1980s. Hedman et al (2011c) found the ripple to extend through the C Ring, and suggested that the tilt was imposed by an impacting stream of rubble, perhaps from a disrupted, 1-10km size, Shoemaker-Levy-9 type object, with an extended node crossing the D and C rings. Hedman et al (2015b) determined, from further analysis, that the event may have had two parts, separated by months. Hedman and Showalter (2016) subsequently found pattern evidence for two other disturbances that occurred in 1979 (in Voyager data) and 2011! Marouf et al (2011) discovered a similar pattern in the C ring, from higher-resolution radio occultation data, that they interpreted as two events, separated by 50 years, that occurred in the late 1300's. It is fascinating that the rings still bear silent witness to these long-lasting scars of cometary impacts. A related example of time variability is ongoing impacts onto the ring by discrete particles large enough to create detectable disturbances – the little cousins of these ripple-forming, comet-size objects. Impacts by meter-size particles have been observed directly; once a leading candidate for triggering spokes (section 4.1.1e), the connection between the observed meter-size impact rates and spoke formation rates has not been pursued in depth. These impact effects were discussed in section 4.1.4b.

The D and C rings show two other, still unexplained, kinds of time variation. Hedman et al (2014c) found that one of the most prominent bright ringlets in the D Ring, also seen by Voyager, is moving inwards at more than 2km/yr, and apparently moved outwards to its current position between Voyager and Cassini. The ringlet also has strong azimuthal clumpiness that seems stable, but cannot be associated with any plausible resonance - with either some known moon, or some known planetary interior modes or rotating structures; all in all it is a puzzling dynamical feature. Also, there are time-variable aspects to several C ring spiral density waves that appear to be driven by density fluctuations fixed to Saturn's internal structure and rotating with its winds – so-called "tesseral" resonances (see section 4.1.1b). Hedman et al (2014a, 2017, 2018b) have found that some of these wavetrains seem to be drifting inwards at about 1km/year, as if the density fluctuations causing them were moving in latitude or depth inside the planet.

4.2.3 F Ring (RC2a) – Focus on F Ring structure, and distribution of associated moonlets or clumps, as sparse observations show clumps, arcs, and possibly transient objects appearing and disappearing.

Because of the strong time variations seen during prime mission, the F Ring became a central focus for Cassini imaging observations during CSM. The F Ring lies about 3000km outside the A Ring edge, and is unique in the family of planetary rings. Faintly glimpsed by Pioneer 11, its kinky, multi-stranded structure was revealed in Voyager images to be dominated by small dust grains, and Voyager radio and stellar occultations showed it to have a very narrow core of larger objects.. Earthbased observations between Voyager and Cassini showed it to be highly variable, with large clumps coming and going, having orbital periods that differed slightly from that of its central strand (McGhee et al 2001). As it was straddled by the 100-km diameter ringmoons Prometheus and Pandora, classical shepherding theory was quickly proposed to explain its survival. However, almost immediately, problems arose with that interpretation, growing over the years when it was realized that not only were the so-called shepherds on chaotic orbits themselves, but objects orbiting between them were excited to even more chaotic orbits. In fact, Cassini very quickly observed some of these objects (2004S6, etc; Porco et al 2005) on orbits that crossed the F Ring, but could not be tracked for more than a few months before they vanished (Cooper et al 2017). Meanwhile, large jets of material were seen splashed out from the central core due to collisions by these careening objects (Charnoz et al 2005, Murray et al 2008, Becker et al 2018), and evidence was found for smaller, unseen objects embedded within the F Ring strands themselves. Dynamical models showed how the perturbations of Prometheus alone could explain the alternating streamer-channel appearance of the F Ring (Murray et al 2005), Buerle et al 2010).

Several new classes of embedded objects were inferred and modeled, based on often faint and initially obscure patterns seen to come and go. “Mini-jets” – small spikes poking out of the central strand – were catalogued and understood as caused by large embedded objects (meters or tens of meters in size perhaps) colliding at low (few m/sec) speeds within the dense central ring strand (Charnoz 2009, Murray et al 2008, Esposito et al 2008, Buerle et al 2010, Albers et al 2012, Meinke et al 2012, Attree et al 2012, 2014). “Fans” or localized, regular brightness fluctuations were shown to be due to small, embedded objects on slightly eccentric orbits relative to the F Ring (Murray et al 2008). Some of these fans were localized to parts of the ring where Prometheus compressed ring material, perhaps actually forming new, small moonlets then and there (Buerle et al 2010).

RSS occultations only detected the F ring’s very narrow (< 1 km) “true core” of cm-and-larger-size particles about 1/3 of the time, showing it had to be azimuthally broken and discontinuous. Using these observations, a new theory was developed in which the stability of the “true core”, in the presence of strong orbital chaos driven locally by Prometheus, was due to a unique overlap of two different kinds of “resonances” (Cuzzi et al 2014, 2018c; see also Albers et al 2012 and Cooper et al 2013). This arrangement of the F Ring’s “true core”, which consists of incomplete “arcs” of macroscopic particles, must occasionally make small adjustments, given the occasional chaotic changes in Prometheus' orbit to which the clumps must readjust. Hedman et al (2011b) observed variations in crystalline ice band depth due to variations in the relative abundance of macroscopic bodies and dust, which have yet to be correlated with the RSS clumping. Large objects forming in “fans”, and usually outside the very

narrowly defined stable true core orbit (Cuzzi et al 2014, 2018c), can become strongly perturbed by Prometheus and evolve into 2004S6-like objects, ultimately recolliding with the F Ring at high speeds. Indeed, while 2004S6 was tracked in 2006-2008 as it collided with the F ring several times and then lost, similar objects have since appeared. Different frequencies and intensities of such big eruptions as seen by Cassini and by Voyager observations underline the sporadic nature of these variations (French et al 2012, 2014).

4.2.4 Ring Age and Origin (RN1a) – Constrain the origin and age of the rings by (a) direct determination of the ring mass, and (b) of the composition of ring ejecta trapped on field lines.

Over the years the ring composition has emerged as perhaps the best gauge of ring age and clue to ring origin. While ring composition is powerfully addressed using traditional remote sensing techniques (section 4.1.2), this objective focused on *in situ* measurements that were only achievable during Cassini's RG and GF orbits.

(a) Determination of ring mass: It was not known, when Cassini was initially planned, that we would be able to obtain a direct measurement of the ring mass; this only became possible in the Cassini Solstice Mission (CSM) GF orbits, when the spacecraft was able to fly between the rings and the planet 22 times. The original AO mission plan was to constrain the ring mass by measuring the ring optical depth and particle size distributions together, and sample all available spiral density waves, using stellar and radio occultations. However, because of the possible ambiguities associated with "hidden mass" in the B ring that arose during the prime mission (section 4.1.1b), six complete close passes were allocated in the GF orbits, during which the spacecraft remained quiet while RSS transmitted a carrier signal to Earth, to allow the small gravitational effects of the rings to be separated from those of Saturn – a mini-Juno mission. The details of the technique, and difficulties encountered, are described by Iess et al (2018) and in this volume. Unexpected and probably azimuthally variable internal properties of the planet (very unlike those of Jupiter) contaminate the gravitational signature of the rings, increasing the measurement uncertainty to perhaps 50% of the signal. It is puzzling that, if the RSS variance is interpreted as internal mass irregularities, the amplitude of these seems considerably larger than would be inferred from the dozen or so spiral density and bending waves currently seen in the rings, that have been identified as being driven by mass fluctuations inside the planet (section 4.1.1b). Nevertheless, it can be concluded with confidence that the ring mass is probably less than the Voyager-era estimate to within the uncertainty (see the RSS team report in this volume and Iess et al 2018). A total ring mass even as large as 0.8 Mimas masses is regarded as unlikely. While RSS has been as yet unable to obtain a radial *profile* of surface mass density, there is a clue from CIRS thermal models that the central B ring region called B3 (105000-110000km) is actually a quite sharply bounded annulus containing 2-3 times the surface mass density of the rest of the B Ring (Reffet et al 2015).

(b) Composition of rings from ring ejecta: The AO mission provided for no direct, in-situ measurement of main ring particle composition; it was planned to rely on remote observations by VIMS and CIRS, and eventually RADAR 2.2cm radiometry, sensing the nonicy component of ring material (see section 4.1.2). Unfortunately, no unambiguous compositional signatures of any materials besides water ice were seen by VIMS, UVIS, or ISS, and other instruments such as

CIRS and RADAR could only constrain the amount of nonicy material in a nonspecific way. Fortunately, in the GF orbits, when Cassini crossed the ring plane inside of the D Ring (and indeed skimmed through the planet's tenuous upper atmosphere) synergistic, dedicated in-situ observations by CDA, INMS, MIMI, and RPWS hit pay dirt.

CDA detected grains at a variety of vertical distances above the rings, with varying silicate/ice fraction (Hsu et al 2018). The Fe/Si ratio suggested low-Fe silicates. The order-unity silicate/Ice ratio in material detected by CDA (especially at high latitudes) is far higher than seen in the main rings or even the more polluted C Ring, and suggests that detected grains have been stripped of most of their ice before detection, perhaps by photosputtering (Hsu et al 2018), but this remains an active area of research. No evidence was found for "free" iron or Fe_xO_y compounds (candidates for reddening the rings; see section 4.1.2a and Cuzzi et al 2009 for a review and discussion), even though their presence *had* been suggested in true interstellar grains detected by CDA (Altobelli et al 2016). CDA observations of organics are expected to be limited to large grains, which were rare because the dust abundance at the radii of ring plane crossings was much lower than had been (conservatively) estimated from spacecraft hazard studies, and most of the detected grains were too tiny to get good mass spectra in the presence of known carbon contamination of CDA. For the larger grains, CDA can say that the concentration of organics is low in any single detected grain, compared to the amount of ice or silicate. Nevertheless, the data are still being analyzed and new results along these lines are anticipated (see, for instance, Hsu et al 2018 and the chapter by the CDA team, this volume).

MIMI detected an equatorial layer of 4-5nm radius grains with vertical thickness of a few thousand km (Mitchell et al 2018) blending into the very rare upper atmosphere of Saturn. These tiny grains plausibly derive from the even flatter D Ring and drift inwards under gas drag while spreading vertically. They are too small to pick up much charge, so orbit at nearly Keplerian speeds, obtaining their few-thousand km vertical thickness by scattering collisions with differentially rotating exospheric H atoms. MIMI could not determine the composition of these grains directly, but estimates their mass flux into the atmosphere at 5kg/s (Mitchell et al 2018 and this volume).

Meanwhile, as Cassini skimmed through the very rarified upper atmosphere on the GF orbits closest to Saturn, INMS detected strong signals due to a very wide range of masses, up to their limit at 100 amu (Waite et al 2018, Perry et al 2018). The abundance of these molecules actually decreased downwards into Saturn, so they are entering from above, not diffusing up from depth. The overall pattern observed is roughly dominated by multiples of carbon atoms, up to C6, but given the likelihood that large molecules fragment into smaller ones within the INMS chamber prior to actually being sampled, detailed inferences require a complex deconvolution process (Miller et al 2018). INMS is unable to detect nonvolatile material like iron or silicates, and is even subject to underestimation of H_2O. The good agreement between the INMS latitudinal signal strength and the thickness of the MIMI 4-5 nm particle layer suggests that the INMS compositions refer to impact fragments of the MIMI particles. Also seen in the INMS spectra are N and O; however, the complexity of the deconvolution leaves some ambiguity about whether the O, N (and even some of the C) were carried as part of the organics or in smaller molecules like NH_3 or CH_4 (Waite et al 2018, Miller et al 2018, Perry et al 2018). For comparison, Cassini VIMS observations see no CH_4 or CO_2 (Cuzzi et al 2009) and STIS spectra see no NH_3 (Cuzzi et al 2018b). INMS estimated a total flux of these materials into Saturn's

upper atmosphere, over a latitudinal band of 5-10^{o} wide, that is about 1000 times larger than the MIMI estimate (Perry et al 2018), and propose that it must be carried dominantly by particles of 1-2nm radius, too small for MIMI to detect but following roughly the same vertical distribution. This flux is so high that INMS suggests it is probably due to a flareup in the D ring, perhaps due to recent activity in the D68 ringlet (Hedman et al 2014c, Hedman and Showalter 2016).

(c) Ring Origin and Age: The age of the rings has been debated since the Voyager era, when two general lines of argument arose suggesting they may be much younger than the solar system. These are described in more detail in several recent review chapters (Cuzzi et al 2009, 2018a; Charnoz et al 2009). First, angular momentum transfer by spiral density waves between the rings and the inner moons should quickly collapse the A ring and spin the close ringmoons outwards, a tidal effect like our own Earth-moon tidal interaction (Goldreich and Tremaine 1982; but see Poulet and Sicardy 2001 or Charnoz et al 2000 for loopholes). Second, pollution of the dominantly icy A and B rings – more than 90% ice, as known since pre-Voyager (Esposito et al 1984; Orton et al 2009) – by dominantly nonicy meteoroid infall should darken them in much less than the age of the solar system (Doyle et al 1989, Cuzzi and Estrada 1998, Elliott and Esposito 2011). It had been argued, however, that the ring mass could be much larger than generally accepted during the Voyager era, because gravitational clumping and lack of sampling by spiral density waves of the most massive (B) ring might allow most of the mass to escape detection (section 4.1.1b). Also, the meteoroid mass flux was very poorly known, and if it had been overestimated by an order of magnitude or so, the rings could remain unpolluted for the age of the solar system.

The combination of ring mass determined by RSS (Iess et al 2018), and the extrinsic meteoroid mass flux measured by CDA (Kempf et al 2018; see section 4.1.4b) at last allows us to constrain the ring age to be less than 250 Myr or so (observational and model-based uncertainties remain) – that is, no older than the dinosaurs. If we must reluctantly relinquish our otherwise physically plausible “primordial ring origin” scenarios, at least there is one plausible “recent origin” scenario, related to a dynamical instability incurred 100Myr ago by a stably evolving Saturn inner moon system (Cuk et al 2018). There are many current issues associated with connecting such an instability (near Rhea’s orbit) and actual formation of a massive ring inside the Roche zone. However, it offers both an independently derived, recent age and also an indication why Saturn is the only giant planet to sport such a young, massive, icy ring. Constraints from cratering of icy moon surfaces and internal evolution will play an important role in testing the idea. The current implications that the rings are colored by organics, that there may be a silicate-rich rubble belt buried within the C Ring (section 4.1.2a) , and even the dark, enigmatic G Ring parent Aegaeon (Hedman et al 2011a) provide important constraints as well.

4.2.5 Ringmoons (RN1b)- Determine the composition of the close-in “ringmoons” as targets of opportunity. *This is discussed in detail in the Final Report of the Icy Satellites Working Group.*

4.2.6 High-resolution Ring Structure and composition (RN1c)- Determine structural and compositional variations at high resolution across selected ring features of greatest interest, using remote and in-situ observations.

A substantial number of new, dedicated observations were prioritized, integrated, and implemented to make use of the unique, up-close-and-personal geometry of Cassini's RG and GF orbits to address "radial structure", meaning on scales larger than the vertical thickness. Also, a large number of ISS 8-15 filter color scans with 3-5km radial resolution were integrated and successfully implemented well before the RG and GF orbits, to address compositional variations, over a large range of illumination and viewing angles, as well as different solar hour angles to assess the role of Saturnshine.

Much higher spatial resolution is needed to assess fine scale structural variations. Recall that the unique SOI observations (400m resolution) were sparsely sampled, were of the unlit face , and were taken at a large relative velocity requiring short exposures. On the other hand, the RG and GF orbits provided similar 100-300m resolution on the lit face as well as of the unlit face, and at low phase angles, with the opportunity to use smear removal tracking. Moreover, one new kind of observation was enabled during the RG and GF orbits – active radar backscattering. Radar observations (from the ground) opened the modern era of Saturn's Rings research 40 years ago, but their sensitivity decreases as distance to the fourth power, so they only became feasible for Cassini in these very close-in geometries. The Radar team did carry out three active radar backscattering radial profiles with the potential to reach several km radial resolution, but reduction of this sort of data has not been previously done by the team and is still in progress (see the chapter by the Radar Team). Indeed, as of this writing, a number of observations taken on the RG and GF orbits remain in the early stages of analysis. However, an overview of high resolution observations by ISS, VIMS, UVIS, and CIRS may be found in Tiscareno and Harris (2018) and Tiscareno et al (2018).

4.2.7 Ring Microstructure (RN2a) - Conduct In-depth studies of ring microstructure such as self-gravity wakes, which permeate the rings. Microstructure has the connotation of structure comparable in scale to the ring vertical thickness (section 4.1.1b). During the CSM, a number of exceptionally high radial resolution scans were implemented of the lit and unlit faces, using smear removal tracking (the so-called "SUPERHRES scans") and targeted observations of, for instance, the Keeler gap in the vicinity of Daphnis, the C Ring plateaus, and other specific regions of interest. Spatial clumping – of several different types and on scales still larger than the expected self-gravity wakes – is widely seen in images with these sub-km resolutions (Tiscareno et al 2018). A number of specially designed "Turnaround" stellar occultations were prioritized and included; these are chord occultations in which the path of the star becomes tangent to the orbital direction at some radius. The implication is that radial stellar velocity vanishes and ultra-high radial resolution can be obtained, along with very good tangential resolution. Finally, the technique of variance analysis[4] has been widely applied and a variety of interesting differences seen from place to place. This sort of analysis is only getting underway (Colwell et al 2018).

4.2.8 New Ring Structures (RN2b) - Perform focused studies of the evolution of newly discovered "propeller" objects. Extend to studies of streaky plateau structure. A dedicated campaign to image selected "giant" propellers (> 1km size) as often as possible was conducted over the last five years of the mission. This campaign yielded several hundred images that successfully targeted propellers, with rich sampling in time. Ongoing analysis of these images

(e.g., section 4.1.3) finds excursions from keplerian orbit of diverse kinds, including both gradual trends and sharp changes of direction. In the RG orbits, three giant propellers were specifically targeted for close-flyby imaging, which successfully revealed their detailed structure. Also in the RG orbits, high-resolution images of the Propeller Belts yielded the first full view of a size distribution in which the largest propellers are 4x to 5x larger than the smallest (Tiscareno et al. 2018). In the GF orbits, images of the plateaus spectacularly confirmed previous suspicions of streaky texture, and further revealed sharp-edged belts of textures (some streaky, some clumpy) at other locations in the main rings (Tiscareno et al. 2018). Most of these data encompass both the lit and unlit faces of the rings, and are still under reduction and analysis.

(5) Saturn "System" Science Results

The possibility of "young rings" now has broadened to the possibility of a young inner icy moon (and ring) system. The evection resonance theory of Cuk et al (2016) not only independently arrives at a similar timescale as ring ages, but also points to Saturn as the most likely planet to incur such a fate. More studies of the icy moon surfaces (especially cratering statistics) are needed to constrain the validity of this hypothesis, and the composition of the moons and rings needs to be taken into account together.

Along these lines, results obtained through the study of rings have led us to a new understanding of the deep interior of Saturn. The discipline, now known as Kronoseismology, is in its infancy, and has led to the suggestion of a diffuse core boundary, and rapidly changing internal structure, at Saturn (section 4.1.1b). Recent results have even shown that the elusive deep interior rotation period of the planet can be determined very precisely by matching internal structure predictions with spiral waves seen in the C Ring.

CDA also detected 46 grains coming from the *Interstellar Flux* stream (its velocity apex or ram direction is known from the velocity of the solar system through the local diffuse Interstellar medium) and constrained their composition (Altobelli et al 2016). This profoundly important *in situ* determination of the composition of ISM grains complements and informs often ambiguous remote sensing determinations (see also section 4.2.4 above). The grains populating the diffuse ISM – those detected here and the most easily studied by remote sensing – include Mg-rich silicates and, perhaps, iron metal or oxides, but are depleted in sulfur. By comparison, the silicates detected by CDA during the GF orbits were also Mg-rich but showed no evidence of companion Fe metal or oxides. The ISM grains were quite homogeneous, probably by repeated processing in the ISM by shocks and radiation. As these grains become embedded in the dark, dense, presolar parent cloud, they accumulate more volatile organics and ices (apparently some sulfur-bearing ices) before flowing into the forming solar system. But, their very refractory mix of silicates and metal would not be expected to change at the low temperatures of these clouds.

(6) Unsolved problems suitable for ongoing research and future missions

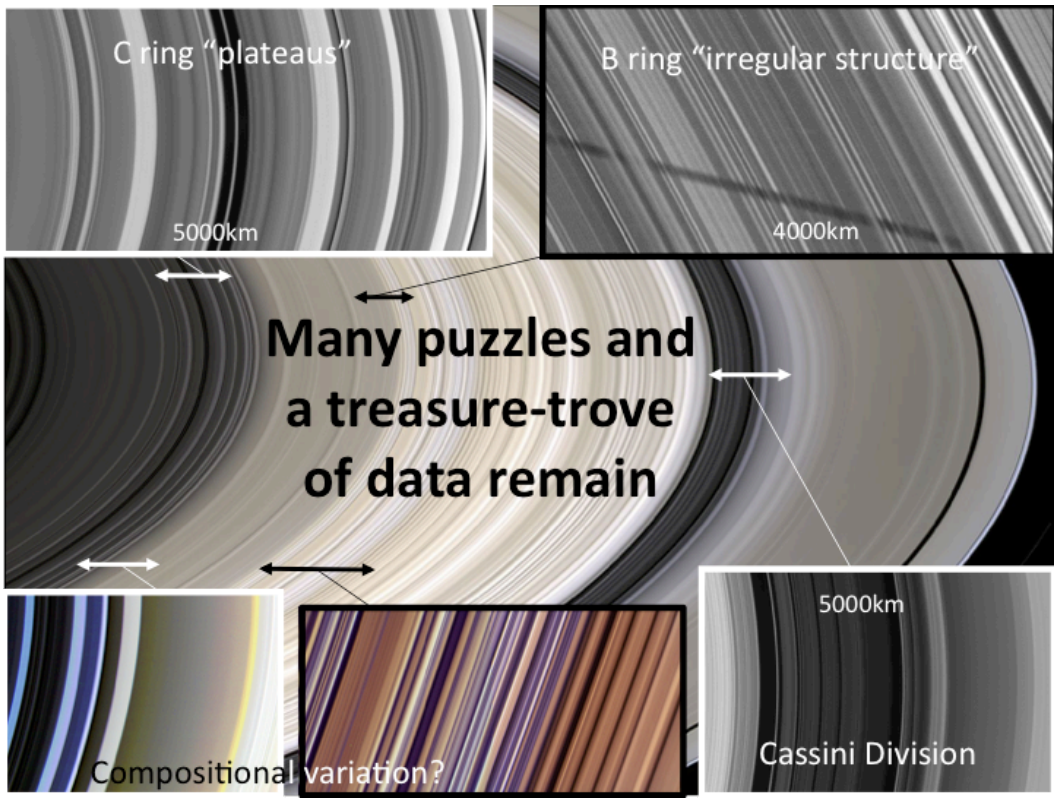

Figure 2: A montage of still-puzzling structure. A mosaic view of Saturn's main rings is shown in the central panel. Certain selected regions are indicated by double-header arrows, and by closeup images shown as insets.

Why is the interior of Saturn so different from that of Jupiter, as seen by the RSS gravity passes, and why are the mass irregularities inferred so different and so much larger than what are inferred from "Kronoseismology" spiral density and bending waves in the rings? Are these differences tied to the faster tidal evolution rates seen for the Saturnian moons than for the jovian moons (the so-called "larger Q" for Jupiter than for Saturn)? What are the embedded mass concentrations responsible for the "tesseral" spiral density waves that rotate at harmonics of Saturn's spin rate, and moreover change with time?

The ring mass and in particular its radial distribution were not as well constrained as hoped, because of unexpected internal structure within Saturn. Only a total ring mass could be determined, and the B ring component inferred by backing out the already very well known A and C Ring masses (from spiral density waves). This remaining uncertainty provides an opportunity for a future mission – to use repeated close gravitational flybys to separate out and fully understand the apparently unusual and intriguing internal structure of the planet, from the radial mass distribution within the rings, hopefully at a few hundred km radial resolution even, to see which parts of the opaque B Ring actually hold how much of the mass. Better radial mass resolution would be useful in the C Ring also, because the possibility that the middle C Ring hides a fossil silicate rubble belt has implications for ring origin; it is currently constrained by a small handful of surface mass densities. There is some evidence that the visual wavelength

spectra of the central C ring differ from the otherwise similar Cassini Division; might this be another clue regarding a buried silicate belt?

The smooth, undulating 80-km scale irregular structure in the inner B ring may be related to ballistic transport, but the array of finer-to-coarser scale structure in the middle and outer B Ring seems to be something different. Could it be some form of viscous overstability, operating at longer wavelengths than models show, and possibly coupling to the even larger scale azimuthal B ring edge variations? In the region between 100,000-104500km, radio and stellar occultations both see successions of very sharp transitions between large and very large optical depth, for which no explanations exist. At the time of this writing, RSS occultations of the very densest B ring regions, taken at the largest ring opening angles where they would be most likely to be even partially transparent, have not been analyzed or released, but are eagerly anticipated.

The outer C Ring hosts a series of 5-8 "plateau" features in optical depth, nearly symmetrically arrayed about the Maxwell gap which is now known to be caused by a 2:1 resonance with the strongest planetary internal vibration mode (Marley and Porco 1993, French et al 2016b, Fuller et al 2014); the reason why a dense, elliptical m=1 ringlet dominates the gap, apparently caused by an m=2 resonance, is not understood. A similar situation occurs at a Titan resonance in the C Ring, but that is an m=1 resonance. The plateaus do not have any special association with resonances from known or predicted planetary internal modes (Marley 2014). They are odd in that their appearance as features is due primarily to locally abrupt changes in particle size distribution rather than surface mass density (sections 4.1.2b, and below). Moreover, ultra-high resolution Cassini images reveal a novel and unique "streaky" structure in the plateaus that is not understood (Tiscareno et al 2018).

Why is there a Cassini Division at all, and *why are there no embedded moonlets clearing its several empty gaps?* It has been suggested that weak perturbations from the fluctuating B Ring edge might play a role (Hedman et al 2010b). Presumably the Cassini Division was originally cleared by a powerful Mimas 2:1 spiral density wave, at a time when the rings were continuous through the region, but how did that early, vigorous evolution lead to today's quiet banded structure? And, how are the moonlet-free C ring gaps formed?

In the A ring, a million "propeller" objects populate three distinct radial belts. *Are these objects transient clumps that emerge from the background material with low, but finite probability and then disperse again?* Giant propellers (found only outside the Encke gap) seem especially hard to create by spontaneous, or triggered formation. Gravitational encounters with smaller masses seem to explain their wandering behavior, but the mass clumps needed are larger than the largest ring particles and even typical self-gravity wakes. There are a few "propeller" objects in the B Ring, but their locations and abundances have not been well characterized. What else could be hiding in the densest parts of the B Ring? What causes the "ghost" gaps in the C ring and outer Cassini Division?

In the F Ring, telltale signatures of embedded, relatively large objects are seen preferentially in strands where they are maximally compressed by Prometheus. If the semimajor axes of these newly created objects lie outside the stable "true core (section 4.2.3), they will develop chaotic orbital perturbations, diffusing away from their formation location as their eccentricity increases, and ultimately recolliding sporadically with the F Ring core. Cycles of such activity may be expected (and there is some evidence from comparing Voyager and

Cassini) but no systematic assessment has been obtained. Meanwhile, even the most recent hypothesis for the stability of the F Ring's true core cannot explain the stable precession of dozens of separated arcs as a single, well defined ellipse. Could the (mostly unconstrained) mass of the F Ring be playing a role?

The systematic increase of the redness of the rings inwards across the B Ring remains a puzzle. In-situ observations (albeit in the D ring) seem to favor large organic molecules, PAHS or fragments of tholins, possibly containing N and maybe even O, as the UV absorber responsible for the ring redness. These red organics seem to be intrinsic to the dominant icy material. Whether or not organics also explain the weaker UV absorption seen in most of the icy moons will be an important clue regarding ring origin scenarios, such as recent ones that connect their origin to a moderately recent collisional erosion/destruction of pre-existing, mature, differentiated icy moons. Can organic material remain associated with liquid water when a moon differentiates, and remain with it when it freezes?

Color and brightness variations within the rings on tens to hundreds of km scale have been interpreted as small-scale, optical-depth dependent regolith grain size variations, but models capable of treating the difficult ring radiative transfer problem have yet to be deployed in compositional analyses. That is, secondary optical-depth dependent effects (like collisional packing or smoothing of particle surfaces) may change the particle phase functions, or volume density effects may change the layer scattering function. Much more analysis needs to be done with more sophisticated, nonclassical radiative transfer models, fitting observations over wide ranges of illumination and viewing geometry, as well as assessing wider ranges of wavelength simultaneously, to understand the situation before compositional implications can be derived with confidence. Shadowing on the surely very ragged ring "particle" surfaces needs to be studied (Cuzzi et al 2017). Also on the subject of radiative transfer models, Cassini's three high-radial-resolution active radar backscattering scans require new models for their interpretation, that can adequately treat coherent backscattering.

Unexplained jumps in particle size distribution are seen at a number of places in the rings where sharp edges appear in optical depth, but across these edges there are only small (or no) contrasts in surface mass density. Basically, this means the "features" are caused by abrupt changes in particle size distribution. The inner edge of the A ring, where it transitions to the Cassini Division, is one such place. The series of C Ring "plateaus", nearly symmetrically surrounding the Maxwell gap (which is known to be associated with a 2:1 resonance with a mode inside Saturn) are like that as well. What causes this effect? Why do the slopes and minimum or maximum sizes in generally powerlaw size distributions of ring particles vary from place to place? Are most particles porous throughout or do they conceal dense, solid cores?

Unexplained microstructure is seen in many places across the rings, at optical depths large and small, in late, high-resolution images which have resolution even better than those taken at SOI, as well as combinations of lit and unlit face geometries, lower smear, and higher signal to noise ratio (Tiscareno et al 2018). The texture can change rather quickly with radius and is not always related to optical depth changes.

The process actually responsible for the initial formation of spokes – whether it be bursts of ionizing radiation from planetary superstorms, magnetic field instabilities, or impacts, remains unclear.

The Ballistic transport process usually believed to explain the sharp inner edges of the A and B Ring, and hypothesized to explain the C ring plateaus, has been modeled assuming the boundaries of these features manifested jumps in surface mass density without particle size changes, and we now know the underlying surface mass density is only slowly varying while the particle size changes abruptly. How do these new realizations affect the models? Could the ejection velocity change from place to place, depending on the nature of the local particle regoliths? How will the results change under new assumptions about meteoroid impact flux and dynamical population? The theory of ring pollution and restructuring by meteoroid bombardment and ballistic transport needs to be tested more carefully against other structures and compositional profiles, and revised to capture more realistic impact outcomes and newly constrained incoming meteoroid fluxes. Matching radial scans of ring color and spectral reflectance with models of compositional evolution must incorporate new understanding about ring surface mass density, particle size, and viscosity. Inclusion of regolith thermal inertias would provide another handle on how particle surfaces respond to meteoroid bombardment.

More sophisticated models of impact chemistry and radiation chemistry are needed – both in micrometeoroid impacts on ring particles, possibly resulting in some C-O chemistry, and by nm-size grain impacts into the INMS entry chamber. INMS sees a variety of molecules – CH_4, CO_2, and NH_3 in particular, that are not evident in VIMS or HST-STIS spectra of the rings. Are some of these created in hypervelocity impacts, transforming absorbing carbon compounds into volatiles or transparent ices? If so (or if not) this would have implications for ring pollution and inferred ring age. *How does the water ice throughout the rings remain crystalline* given constant radiation and meteoroid bombardment? VIMS spectral and occultation observations strongly support crystalline ice.

Explanation for the geologically recent formation of the rings: We now have a new set of constraints, and even an appealing theoretical hypothesis to explore; however, we are still lacking a complete understanding as to how the rings formed in their current location, within Saturn's Roche limit, from a differentiated icy object with a trace, intimately mixed organic component, 250 Myr ago, even given disruptive collisions near the current orbit of Rhea. Observations and interpretation of icy moon surfaces can contribute meaningful constraints.

… Coda …

This short review can in no way capture the depth and complexity of the analysis that has gone into every one of the incomplete list of 200 publications cited here, each of them several years work for multiple scientists. Each of these papers has contributed one critical and unique stone to the edifice of knowledge we now possess about the rings of Saturn – stones all formed from bits returned by Cassini's spectacular 13 year mission. Nor can it adequately convey the even larger and deeper, still unanalyzed and uninterpreted amount of data so thoughtfully conceived, passionately argued for, painstakingly planned, obtained, carefully calibrated, and stored in the Planetary Data System that awaits the attention of future generations of ring scientists. But, we hope it can provide an idea of the scope of where we stand today, and hints at future directions of research. Even this summary would be different if it were written a year from now. The Cassini Rings Discipline Working Group has nothing but admiration and deep appreciation for the dedication of the hundreds of engineers and dozens of managers at JPL who made this mission possible, some of whom may be lucky enough to return to Saturn on a future mission and help answer these outstanding questions.

References

Albers, N.; Sremčević, M.; Colwell, J. E.; Esposito, L. W. (2012) Saturn's F ring as seen by Cassini UVIS: Kinematics and statistics; Icarus 217, 367-388.

Altobelli, N.; Postberg, F.; Fiege, K.; Trieloff, M.; Kimura, H.; Sterken, V. J.; Hsu, H.-W.; Hillier, J.; Khawaja, N.; Moragas-Klostermeyer, G.; Blum, J.; Burton, M.; Srama, R.; Kempf, S.; Gruen, E. (2016) Flux and composition of interstellar dust at Saturn from Cassini's Cosmic Dust Analyzer; Science, 352, 312-318

Attree, N. O.; Murray, C. D.; Cooper, N. J.; Williams, G. A. (2012) Detection of Low-velocity Collisions in Saturn's F Ring; ApJL 755, Issue 2, article id. L27

Attree, N. O.; Murray, C.D.; Williams, G. A.; Cooper, N. J. (2014) A survey of low-velocity collisional features in Saturn's F ring; Icarus, 227, 56-66.

Baillié, K.; Colwell, J. E.; Lissauer, J.J.; Esposito, L. W.; Sremčević, M. (2011) Waves in Cassini UVIS stellar occultations. 2. The C ring; Icarus 216, 292-308.

Baillié, K.; Colwell, J. E.; Esposito, L. W.; Lewis, M. C. (2013) Meter-sized Moonlet Population in Saturn's C Ring and Cassini Division; Astron. J. 145, Issue 6, article id. 171, 10 pp.

Becker, T. M.; Colwell, J. E.; Esposito, L. W.; Bratcher, A. D. (2016) Characterizing the particle size distribution of Saturn's A ring with Cassini UVIS occultation data; Icarus 279, 20-35.

Becker, T. M.; Colwell, J.E.; Esposito, L. W.; Attree, N.O.; Murray, C.D. (2018) Cassini UVIS solar occultations by Saturn's F ring and the detection of collision-produced micron-sized dust; Icarus 306, 171-199.

Beurle, K.; Murray, C. D.; Williams, G. A.; Evans, M. W.; Cooper, N. J.; Agnor, C. B. (2010) Direct Evidence for Gravitational Instability and Moonlet Formation in Saturn's Rings; ApJ 718, L176-L180

Borderies, N.; Goldreich, P.; Tremaine, S. (1985) A granular flow model for dense planetary rings; Icarus 63, 406-420.

Bradley, E. T.; Colwell, J. E.; Esposito, L. W.; Cuzzi, J. N.; Tollerud, H.; Chambers, L. (2010) Far ultraviolet spectral properties of Saturn's rings from Cassini UVIS; Icarus 206, 458-466.

Bradley, E. T.; Colwell, J. E.; Esposito, L. W. (2013) Scattering properties of Saturn's rings in the far ultraviolet from Cassini UVIS spectra; Icarus 225, 726-739.

Bromley, B. C.; Kenyon, S. J. (2013) Migration of Small Moons in Saturn's Rings; ApJ 764, Issue 2, article id. 192

Burns, J. A.; Showalter, M. R.; Morfill, G. E. (1984) The ethereal rings of Jupiter and Saturn; IN: Planetary rings (A85-34401 15-88). Tucson, AZ, University of Arizona Press, 200-272.

Burns, J. A.; Schaffer, L. E.; Greenberg, R. J.; Showalter, M. R. (1985) Lorentz resonances and the structure of the Jovian ring; Nature 316, 115-119.

Chambers, L. S.; Cuzzi, J. N.; Asphaug, E.; Colwell, J.; Sugita, S. (2008) Hydrodynamical and radiative transfer modeling of meteoroid impacts into Saturn's rings; Icarus 194, 623-635.

Charnoz, S. (2009) Physical collisions of moonlets and clumps with the Saturn's F-ring core; Icarus 201, 191-197.

Charnoz, S.; Dones, L.; Esposito, L. W.; Estrada, P.R.; Hedman, M. M. (2009) Origin and Evolution of Saturn's Ring System; in Saturn from Cassini-Huygens, by Dougherty, M. K.; Esposito, L.W.; Krimigis, S.M., ISBN 978-1-4020-9216-9. Springer Science+Business Media B.V., 2009, p. 537

Charnoz, S.; Porco, C. C.; Déau, E.; Brahic, A.; Spitale, J. N.; Bacques, G.; Baillie, K. (2005) Cassini Discovers a Kinematic Spiral Ring Around Saturn; Science 310, 1300-1304

Charnoz, S. Salmon, J.; Crida, A. (2010) The recent formation of Saturn's moonlets from viscous spreading of the main rings; Nature, 465, 752-754

Charnoz, S. R. M. Canup, A. Crida and L. Dones (2018) The Origin of Planetary Ring Systems; a chapter in "Planetary Rings": M. Tiscareno and C. Murray, eds. (Cambridge) p. 515-536

Ciarniello, M. E. A. (2018), Cassini-VIMS observations of Saturn's main rings: II. A spectrophotometric study by means of Monte Carlo ray-tracing and Hapke's theory (in preparation), Icarus, in review.

Clark, R. N.; Cruikshank, D. P.; Jaumann, R.; Brown, R. H.; Stephan, K.; Dalle Ore, C. M.; Eric Livo, K.; Pearson, N.; Curchin, J. M.; Hoefen, T. M.; Buratti, B. J.; Filacchione, G.; Baines, K.H.; Nicholson, P.D. (2012) The surface composition of Iapetus: Mapping results from Cassini VIMS; Icarus, 218, 831-860.

Colwell, J. E., Esposito, L. W., and Sremčević, M. 2006. Self-gravity wakes in Saturn’s A ring measured by stellar occultations from Cassini. Geophys. Res. Lett., 33, L07201.

Colwell, J. E.; Esposito, L. W.; Sremčević, M.; Stewart, G. R.; McClintock, W. E. (2007) Self-gravity wakes and radial structure of Saturn's B ring; Icarus 190, 127-144.

Colwell, J. E.; Nicholson, P. D.; Tiscareno, M. S.; Murray, C. D.; French, R. G.; Marouf, E. A. (2009) The Structure of Saturn's Rings; in Dougherty M.K., Esposito L.W., and Krimigis S.M., eds, (2009); ``Saturn from Cassini-Huygens"; Springer. ISBN 978-1-4020-9216-9

Colwell, J. E.; Esposito, L. W.; Cooney, J. H. (2018) Particle sizes in Saturn's rings from UVIS stellar occultations 1. Variations with ring region; Icarus, 300, 150-166.

Connerney, J. E. P.; Waite, J. H. (1984) New model of Saturn's ionosphere with an influx of water from the rings; Nature 312, 136-138.

Cooper, N. J.; Murray, C. D.; Williams, G. A. (2013) Local Variability in the Orbit of Saturn's F Ring; Astron. J. 145, Issue 6, article id. 161, 15 pp.

Cooper, N. J., C. D. Murray, and S. Renner (2017) F Ring Objects; presented at Cassini End of Mission PSG; Pasadena, CA, September 16, 2017

Crida, A.; Papaloizou, J. C. B.; Rein, H.; Charnoz, S.; Salmon, J. (2010) Migration of a Moonlet in a Ring of Solid Particles: Theory and Application to Saturn's Propellers; AJ 140, 944-953

Cuzzi, J. N.; Estrada, P. R. (1998) Compositional Evolution of Saturn's Rings Due to Meteoroid Bombardment; Icarus 132, 1-35.

Cuzzi, J.; Clark, R.; Filacchione, G.; French, R.; Johnson, R.; Marouf, E.; Spilker, L. (2009): in Dougherty M.K., Esposito L.W., and Krimigis S.M., eds, (2009); ``Saturn from Cassini-Huygens"; Springer. ISBN 978-1-4020-9216-9; p. 459

Cuzzi, J. N.; Burns, J. A.; Charnoz, S.; Clark, R. N.; Colwell, J. E.; Dones, L.; Esposito, L. W.; Filacchione, G.; French, R. G.; Hedman, M. M.; Kempf, S.; Marouf, E. A.; Murray, C. D.; Nicholson, P. D.; Porco, C. C.; Schmidt, J.; Showalter, M. R.; Spilker, L. J.; Spitale, J. N.; Srama, R.; Sremčević, M.; Tiscareno, M. S.; Weiss, J. (2010) An Evolving View of Saturn’s Dynamic Rings; Science, 327, 1470-1475

Cuzzi, J. N.; Whizin, A. D.; Hogan, R. C.; Dobrovolskis, A. R.; Dones, L.; Showalter, M. R.; Colwell, J. E.; Scargle, J. D. (2014) Saturn’s F Ring core: Calm in the midst of chaos; Icarus 232, 157-175.

Cuzzi, J. N.; Chambers, L. B.; Hendrix, A. R. (2017) Rough surfaces: Is the dark stuff just shadow?; Icarus 289, 281-294.

Cuzzi, J. N., G. Filacchione, and E. A. Marouf et al (2018a) Saturn's Rings; a chapter in ``Planetary Rings": M. Tiscareno and C. Murray, eds. (Cambridge)

Cuzzi, J. N.; French, R.G.; Hendrix, A. R.; Olson, D. M.; Roush, T.; Vahidinia, S. (2018b) HST-STIS spectra and the redness of Saturn's rings; Icarus 309, 363-388.

Cuzzi, J. N., E. A. Marouf, R. G. French, R.A. Jacobson, C. D. Murray, and N. J. Cooper (2018c) Saturn's F Ring is shepherded by Prometheus; in review, Science Advances

D'Aversa, E., G. Bellucci, P. D. Nicholson, M. M. Hedman, R. H. Brown, M. R. Showalter, F. Altieri, F. G. Carrozzo, G. Filacchione, and F. Tosi (2010), The spectrum of a Saturn ring spoke from Cassini/VIMS, GRL, 37(1)

Déau, E.; Dones, L.; Charnoz, S.; West, R. A.; Brahic, A.; Decriem, J.; Porco, C. C. (2013) The opposition effect in Saturn's main rings as seen by Cassini ISS: 1. Morphology of phase functions and dependence on the local optical depth; Icarus, 226, 591-603.

Déau, E. (2015) The opposition effect in Saturn's main rings as seen by Cassini ISS: 2. Constraints on the ring particles and their regolith with analytical radiative transfer models; Icarus, 253, 311-345.

Déau, E.; Dones, L.; Mishchenko, M. I.; West, R. A.; Helfenstein, P.; Hedman, M. M.; Porco, C.C. (2018) The opposition effect in Saturn's main rings as seen by Cassini ISS: 4. Correlations of the surge morphology with surface albedos and VIMS spectral properties; Icarus 305, 324-349.

Dougherty, M. et al (2018) Science, submitted

Doyle, L. R.; Dones, L.; Cuzzi, J. N. (1989) Radiative transfer modeling of Saturn's outer B ring; Icarus 80, 104-135.

Durisen, R. H.; Cramer, N. L.; Murphy, B. W.; Cuzzi, J. N.; Mullikin, T. L., Cederbloom, S. E. (1989) Ballistic transport in planetary ring systems due to particle erosion mechanisms. I - Theory, numerical methods, and illustrative examples; Icarus 80, 136-166.

Durisen, R.H.; Bode, P. W.; Cuzzi, J. N.; Cederbloom, S. E.; Murphy, B. W. (1992) Ballistic transport in planetary ring systems due to particle erosion mechanisms. II - Theoretical models for Saturn's A- and B-ring inner edges; Icarus 100, 364-393.

Elliott, J. P.; Esposito, L. W. (2011) Regolith depth growth on an icy body orbiting Saturn and evolution of bidirectional reflectance due to surface composition changes; Icarus 2012, 268-274.

El Moutamid, M.; Nicholson, P.D.; Hedman, M. M.; Gierasch, P. J.; Burns, J. A.; French, R. G. (2016a) Tesseral resonances in the rings of Saturn; AAS/DDA meeting #47, id.400.05

El Moutamid, M.; Hedman, M. M.; Nicholson, P. D.; Gierasch, P.J.; Burns, J. A. (2016b) Evidence of differential rotation inside Saturn from waves of its rings; AAS/DPS meeting #48, id.114.0

El Moutamid, M., P. D. Nicholson, R. G. French, M. S. Tiscareno, C. D. Murray, M. W. Evans, C. M. French, M. M. Hedman, and J. A. Burns (2016c), How Janus' orbital swap affects the edge of Saturn's A ring?, Icarus, 279, 125-140

Elrod, M. K.; Tseng, W.-L.; Woodson, A. K.; Johnson, R. E. (2014) Seasonal and radial trends in Saturn's thermal plasma between the main rings and Enceladus; Icarus 242, 130-137

Esposito, L. W.; Meinke, B. K.; Colwell, J. E.; Nicholson, P.D.; Hedman, M.M. (2008) Moonlets and clumps in Saturn's F ring; Icarus 194, 278-289.

Esposito, L. W.; Albers, N.; Meinke, B. K.; Sremcevic, M.; Madhusudhanan, P.; Colwell, J. E.; Jerousek, R. G. (2012) A predator-prey model for moon-triggered clumping in Saturn's rings; Icarus 217, 103-114.

Estrada, P. R.; Durisen, R. H.; Cuzzi, J. N.; Morgan, D.A. (2015) Combined structural and compositional evolution of planetary rings due to micrometeoroid impacts and ballistic transport; Icarus 252, 415-439.

Estrada, P. R., R. H. Durisen, and H. N. Latter (2018) Meteoroid Bombardment and Ballistic Transport in Planetary Rings; in "Planetary Rings": M. Tiscareno and C. Murray, eds. (Cambridge) p. 198-224

Ferrari, C., Brooks, S., Edgington, S., *et al.* 2009. Structure of self- gravity wakes in Saturn's A ring as measured by Cassini CIRS. *Icarus*, **199**, 145–153.

Filacchione, G.; Capaccioni, F.; Ciarniello, M.; Clark, R. N.; Cuzzi, J. N.; Nicholson, P. D.; Cruikshank, D. P.; Hedman, M. M.; Buratti, B. J.; Lunine, J. I.; Soderblom, L. A.; Tosi, F.; Cerroni, P.; Brown, R. H.; McCord, T. B.; Jaumann, R.; Stephan, K.; Baines, K. H.; Flamini, E. (2012) Saturn's icy satellites and rings investigated by Cassini-VIMS: III - Radial compositional variability; Icarus 220, 1064-1096.

Filacchione, G.; Capaccioni, F.; Clark, R. N.; Nicholson, P. D.; Cruikshank, D. P.; Cuzzi, J. N.; Lunine, J. I.; Brown, R. H.; Cerroni, P.; Tosi, F.; Ciarniello, M.; Buratti, B. J.; Hedman, M. M.; Flamini, E. (2013) The Radial Distribution of Water Ice and Chromophores across Saturn's System; ApJ 766, Issue 2, article id. 76

Filacchione, G.; Ciarniello, M.; Capaccioni, F.; Clark, R. N.; Nicholson, P. D.; Hedman, M. M.; Cuzzi, J. N.; Cruikshank, D. P.; Dalle Ore, C. M.; Brown, R. H.; Cerroni, P.; Altobelli, N.; Spilker, L. J. (2014) Cassini-VIMS observations of Saturn's main rings: I. Spectral properties and temperature radial profiles variability with phase angle and elevation; Icarus 241, 45-65.

Flandes, A., *et al.* 2010. Brightness of Saturn's rings with decreasing solar elevation. *Planet. Space Sci.*, **58**, 1758–1765.

French, R. S.; Showalter, M. R.; Sfair, R.; Argüelles, C. A.; Pajuelo, M.; Becerra, P.; Hedman, M. M.; Nicholson, P. D. (2012) The brightening of Saturn's F ring; Icarus, 219, 181-193.

French, R.S.; Hicks, S. K.; Showalter, M. R.; Antonsen, A. K.; Packard, D. R. (2014) Analysis of clumps in Saturn's F ring from Voyager and Cassini; Icarus, 241, 200-220.

French, R. G.; Marouf, E.A.; Rappaport, N.J.; McGhee, C. A. (2010) Occultation Observations of Saturn's B Ring and Cassini Division; AJ 139, 1649-1667

French, R.G.; Nicholson, P.D.; McGhee-French, C. A.; Lonergan, K.; Sepersky, T.; Hedman, M. M.; Marouf, E.A.; Colwell, J. E. (2016a) Noncircular features in Saturn's rings III: The Cassini Division; Icarus 274, 131-162.

French, R.G.; Nicholson, P. D.; Hedman, M. M.; Hahn, J.M.; McGhee-French, C. A.; Colwell, J. E.; Marouf, E. A.; Rappaport, N. J. (2016b) Deciphering the embedded wave in Saturn's Maxwell ringlet; Icarus 279, 62-77.

Fuller, J. (2014) Saturn ring seismology: Evidence for stable stratification in the deep interior of Saturn; Icarus 242, 283-296.

Fuller, J.; Luan, J.; Quataert, E. (2016) Resonance locking as the source of rapid tidal migration in the Jupiter and Saturn moon systems; MNRAS 458, 3867-3879

Goldreich, P.; Tremaine, S. (1980) Disk-satellite interactions; ApJ 241, 425-441.

Goldreich, P.; Tremaine, S. (1982) The dynamics of planetary rings; Ann. Revs. Astron. Astrophys. 20. 249-283.

Gurnett, D. A.; Kurth, W. S.; Hospodarsky, G. B.; Persoon, A. M.; Xin, L.; Farrell, W.; Lecacheux, A.; Wahlund, J.-E. (2004) Cassini Observations of Radio and Plasma Wave Phenomena Associated with the Saturn's Rings; AAS/DPS meeting #36, id.02.04; BAAS 36, p.1067

Harbison, R. A.; Nicholson, P. D.; Hedman, M. M. (2013) The smallest particles in Saturn’s A and C Rings; Icarus 226, 1225-1240.

Hedman, M. M., *et al. (*2007a) Self-gravity wake structures in Saturn’s A ring revealed by Cassini VIMS. *Astron. J.*, **133**, 2624–2629.

Hedman, M. M., et al. (2007b) Saturn's dynamic D ring; Icarus, 188, 89-107

Hedman, M. M.; Burns, J. A.; Tiscareno, M. S.; Porco, C. C. (2009a) Organizing some very tenuous things: Resonant structures in Saturn's faint rings; Icarus 202, 260-279.

Hedman, M. M.; Murray, C. D.; Cooper, N. J.; Tiscareno, M. S.; Beurle, K.; Evans, M. W.; Burns, J. A. (2009b) Three tenuous rings/arcs for three tiny moons; Icarus 199, 378-386.

Hedman, M. M.; Burt, J. A.; Burns, J. A.; Tiscareno, M. S. (2010a) The shape and dynamics of a heliotropic dusty ringlet in the Cassini Division; Icarus 210, 284-297.

Hedman, M. M.; Nicholson, P. D.; Baines, K. H.; Buratti, B. J.; Sotin, C.; Clark, R. N.; Brown, R. H.; French, R. G.; Marouf, E. A. (2010b) The Architecture of the Cassini Division ; AJ 139, 228-251

Hedman, M. M.; Cooper, N. J.; Murray, C. D.; Beurle, K.; Evans, M. W.; Tiscareno, M. S.; Burns, J. A. (2010c) Aegaeon (Saturn LIII), a G-ring object; Icarus 207, 433-447.

Hedman, M. M.; Burns, J. A.; Thomas, P. C.; Tiscareno, M. S.; Evans, M. W. (2011a) Physical properties of the small moon Aegaeon (Saturn LIII); EPSC-DPS Joint Meeting 2011, October 2011a, Nantes, France.

Hedman, M. M.; Nicholson, P. D.; Showalter, M. R.; Brown, R. H.; Buratti, B. J.; Clark, R. N.; Baines, K.; Sotin, C. (2011b) The Christiansen Effect in Saturn's narrow dusty rings and the spectral identification of clumps in the F ring; Icarus 215, 695-711. [Erratum: 2012Icar..218..735H]

Hedman, M. M.; Burns, J. A.; Evans, M. W.; Tiscareno, M. S.; Porco, C. C. (2011c) Saturn's Curiously Corrugated C Ring ; Science 332, 708.

Hedman, M. M.; Burns, J. A.; Hamilton, D. P.; Showalter, M. R. (2012) The three-dimensional structure of Saturn's E ring; Icarus 217, 322-338.

Hedman, M. M.; Nicholson, P. D. (2013a) Kronoseismology: Using Density Waves in Saturn's C Ring to Probe the Planet's Interior; AJ 146, article id. 12, 16 pp.

Hedman, M. M.; Nicholson, P. D.; Cuzzi, J. N.; Clark, R. N.; Filacchione, G.; Capaccioni, F.; Ciarniello, M. (2013b) Connections between spectra and structure in Saturn's main rings based on Cassini VIMS data; Icarus 223, 105-130.

Hedman, M. M.; Burns, J. A.; Hamilton, D. P.; Showalter, M. R. (2013c) Of horseshoes and heliotropes: Dynamics of dust in the Encke Gap; Icarus 223, 252-276.

Hedman, M. M.; Nicholson, P. D. (2014a) More Kronoseismology with Saturn's rings; MNRAS 444, 1369-1388

Hedman, M. M., P. D. Nicholson, and H. Salo (2014b), Exploring Overstabilities in Saturn's A Ring Using Two Stellar Occultations, AJ, 148, 15, doi:10.1088/0004-6256/148/1/15.

Hedman, M. M.; Burt, J. A.; Burns, J. A.; Showalter, M. R. (2014c) Non-circular features in Saturn's D ring: D68; Icarus 233, 147-162.

Hedman, M, M.; Stark, C, C. (2015) Saturn's G and D Rings Provide Nearly Complete Measured Scattering Phase Functions of Nearby Debris Disks; ApJ 811, Issue 1, article id. 67

Hedman, M. M.; Burns, J. A.; Showalter, M. R. (2015b) Corrugations and eccentric spirals in Saturn's D ring: New insights into what happened at Saturn in 1983; Icarus 248, 137-161.

Hedman, M. M.; Nicholson, P. D. (2016) The B-ring's surface mass density from hidden density waves: Less than meets the eye? Icarus 279, 109-124.

Hedman, M. M.; Showalter, M. R. (2016) A new pattern in Saturn's D ring created in late 2011; Icarus 279, 155-165.

Hedman, M. M.; El Moutamid, M.; Nicholson, P. D. (2017) Drifting waves in Saturn's C ring, evidence for changes in Saturn's interior; AAS/DDA meeting #48, id.401.03

Hedman, M. M., F. Postberg, D. P. Hamilton, S. Renner, and H.-W. Hsu (2018a) Dusty Rings; a chapter in "Planetary Rings": M. Tiscareno and C. Murray, eds. (Cambridge) p. 308-335

Hedman, M. M.; Nicholson, P. D.; El Moutamid, M. (2018b) Evidence for Changes in Saturn's Interior from Structures in Its Rings; 49th LPSC, No. 2083, id.1288

Horanyi, M.; Burns, J. A.; Hedman, M. M.; Jones, G. H.; Kempf, S. (2009) Diffuse Rings; in Saturn from Cassini-Huygens, by Dougherty, M.K.; Esposito, L. W.; Krimigis, S. M., ISBN 978-1-4020-9216-9. Springer Science+Business Media B.V., 2009, p. 511

Hsu et al (2018) Science, submitted

Iess et al (2018) Science, submitted

Jacobson, R. A.; Spitale, J.; Porco, C. C.; Beurle, K.; Cooper, N. J.; Evans, M. W.; Murray, C. D. (2008) Revised Orbits of Saturn's Small Inner Satellites; Astron. J. 135, 261-263

Jerousek, R. G.; Colwell, J.E.; Esposito, L.W.; Nicholson, P. D.; Hedman, M. M. (2016) Small particles and self-gravity wakes in Saturn's rings from UVIS and VIMS stellar occultations; Icarus 279, 36-50.

Johnson, R.E.; Tseng, W.-L.; Elrod, M. K.; Persoon, A. M. (2017) Nanograin Density Outside Saturn’s A Ring; ApJL 834, Issue 1, article id. L6

Kempf et al 2018, in preparation (mass flux paper)

Laughlin, G.; Korchagin, V.; Adams, F. C. (1997) Spiral Mode Saturation in Self-Gravitating Disks; ApJ 477, 410-423.

Lainey, V.; Jacobson, R. A.; Tajeddine, R.; Cooper, N. J.; Murray, C.; Robert, V.; Tobie, G.; Guillot, T.; Mathis, S.; Remus, F.; Desmars, J.; Arlot, J.-E.; De Cuyper, J.-P.; Dehant, V.; Pascu, D.; Thuillot, W.; Le Poncin-Lafitte, C.; Zahn, J.-P. (2017) New constraints on Saturn's interior from Cassini astrometric data; Icarus 281, 286-296.

Leyrat, C., Spilker, L. J., Altobelli, N., Pilorz, S., and Ferrari, C. 2008. Infrared observations of Saturn's rings by Cassini CIRS: Phase angle and local time dependence. *Planet. Space Sci.*, **56**, 117–133.

Mankovich, C., M.S. Marley, J. J. Fortney, and N. Movshovitz (2018) Cassini Ring Seismology as a Probe of Saturn's Interior I: Rigid Rotation; Submitted to ApJ

Marley, M, S. (1990) Nonradial oscillations of Saturn: Implications for ring system structure; Ph.D. Thesis, Univ. of Arizona, Tucson

Marley, M. S.; Hubbard, W. B.; Porco, C. C. (1987) Saturnian Nonradial p - Mode Oscillations and C Ring Structure; BAAS 19, p.889

Marley, M. S.; Hubbard, W. B.; Porco, C. C. (1989) C-Ring Features and f-Mode Oscillations of Saturn; BAAS 21, p.928

Marley, M. S.; Porco, C. C. (1993) Planetary acoustic mode seismology - Saturn's rings; Icarus 106, 508

Marley, M. S. (2014) Saturn ring seismology: Looking beyond first order resonances; Icarus 234, 194-199.

Marouf, E. A.; French, R. G.; Rappaport, N. J.; Wong, K.; McGhee, C.; Anabtawi, A. (2011) Six Centuries Old Spiral of Vertical Corrugations in Saturn's C-Ring; AGU Fall Meeting 2011, abstract id.P12B-01

McGhee, C. A.; Nicholson, P. D.; French, R. G.; Hall, K. J. (2001) HST Observations of Saturnian Satellites during the 1995 Ring Plane Crossings; Icarus 152, 282-315

McGhee, C. A.; French, R. G.; Dones, L.; Cuzzi, J. N.; Salo, H. J.; Danos, R. (2005) HST observations of spokes in Saturn's B ring; Icarus 173, 508-521.

Meinke, B. K.; Esposito, L. W.; Albers, N.; Sremčević, M. (2012) Classification of F ring features observed in Cassini UVIS occultations; Icarus 218, 545-554.

Miller et al 2018 Science, submitted

Mitchell, C. J.; Horányi, M.; Havnes, O.; Porco, C. C. (2006) Saturn's Spokes: Lost and Found; Science 311, 1587-1589

Mitchell, C. J.; Porco, C. C.; Dones, H. L.; Spitale, J. N. (2013) The behavior of spokes in Saturn's B ring; Icarus 225, 446-474.

Mitchell, C. J.; Porco, C. C.; Weiss, J. W. (2015) Tracking the Geysers of Enceladus into Saturn's E Ring; AJ 149, Issue 5, article id. 156, 16 pp. (2015).

Mitchell, D. et al 2018 Scence, submitted

Morishima, R., Spilker, L., Salo, H., *et al.* 2010. A multilayer model for thermal infrared emission of Saturns rings II: Albedo, spins, and vertical mixing of ring particles inferred from Cassini CIRS. *Icarus*, **210**, 330–345.

Morishima, R., G., Edgington S., and Spilker, L. 2012. Regolith grain sizes of Saturn's rings inferred from Cassini-CIRS far-infrared spectra. *Icarus*, **221**, 888–899.

Morishima, R., Spilker, L., and Truner, N. 2014. Azimuthal temperature modulations of Saturn's A ring caused by self-gravity wakes. *Icarus*, **228**, 247–259.

Morishima, R., Spilker, L., Brooks, S., Deau, E., and Pilorz, S. 2016. Incomplete cooling down of Saturn's A ring at solar equinox: Implication for seasonal thermal inertia and internal structure of ring particles. *Icarus*, **279**, 2–19.

Murray, C. D.; Chavez, C.; Beurle, K.; Cooper, N.; Evans, M. W.; Burns, J. A.; Porco, C. C. (2005) How Prometheus creates structure in Saturn's F ring; Nature 437, 1326-1329

Murray, C.D.; Beurle, K.; Cooper, N.J.; Evans, M. W.; Williams, G. A.; Charnoz, S. (2008) The determination of the structure of Saturn's F ring by nearby moonlets; Nature, 453, 7196, 739-744

Murray, C. D. and R. C. French (2018) The F Ring; a chapter in "Planetary Rings": M. Tiscareno and C. Murray, eds. (Cambridge) p. 336-360

Nicholson, P. D.; Hedman, M. M.; Clark, R. N.; Showalter, M. R.; Cruikshank, D. P.; Cuzzi, J. N.; Filacchione, G.; Capaccioni, F.; Cerroni, P.; Hansen, G.B.; Sicardy, B.; Drossart, P.; Brown, R. H.; Buratti, B.J.; Baines, K. H.; Coradini, A. (2008) A close look at Saturn's rings with Cassini VIMS; Icarus, 193, 182-212.

Nicholson, P. D.; Hedman, M. M. (2010) Self-gravity wake parameters in Saturn's A and B rings; Icarus 206, 410-423.

Nicholson, P.D., R.G. French, M.M. Hedman, *et al*. (2014): "Noncircular features in Saturn's rings I: The edge of the B ring." *Icarus* **227**, 152-175.

Nicholson, P. D.; R. G. French, and J. N. Spitale (2018) Narrow Rings, Gaps and Sharp Edges; in "Planetary Rings": M. Tiscareno and C. Murray, eds. (Cambridge) p. 276-307

Nitter, T.; Havnes, O.; Melandsø, F. (1998) Levitation and dynamics of charged dust in the photoelectron sheath above surfaces in space; JGR 103, 6605-6620

Orton, G. S.; Baines, K. H.; Cruikshank, D.; Cuzzi, J. N.; Krimigis, S. M.; Miller, S.; Lellouch, E. (2009) Review of Knowledge Prior to the Cassini-Huygens Mission and Concurrent Research; in Saturn from Cassini-Huygens, by Dougherty, M. K.; Esposito, L. W.; Krimigis, S. M., ISBN 978-1-4020-9216-9. Springer Science+Business Media B.V., 2009, p. 9

Pan, M.; Chiang, E. (2010) The Propeller and the Frog; ApJL 722, L178-L182

Pan, M.; Chiang, E. (2012) Care and Feeding of Frogs; AJ 143, Issue 1, article id. 9, 6 pp.

Pan, M.; Rein, H.; Chiang, E. Evans, S.N. (2012) Stochastic flights of propellers; MNRAS 427, 2788-2796.

Pilorz, S., Altobelli, N., Colwell, J., and Showalter, M. 2015. Thermal transport in Saturn's B ring inferred from Cassini CIRS. *Icarus*, **254**, 157–177.

Porco, C.; Danielson, G. E.; Goldreich, P.; Holberg, J. B.; Lane, A. L. (1984) Saturn's nonaxisymmetric ring edges at 1.95 R(s) and 2.27 R(s); Icarus 60, 17-28.

Porco, C. C.; Baker, E.; Barbara, J.; Beurle, K.; Brahic, A.; Burns, J. A.; Charnoz, S.; Cooper, N.; Dawson, D. D.; Del Genio, A. D.; Denk, T.; Dones, L.; Dyudina, U.; Evans, M. W.; Giese, B.; Grazier, K.; Helfenstein, P.; Ingersoll, A. P.; Jacobson, R. A.; Johnson, T. V.; McEwen, A.; Murray, C. D.; Neukum, G.; Owen, W. M.; Perry, J.; Roatsch, T.; Spitale, J.; Squyres, S.; Thomas, P.; Tiscareno, M.; Turtle, E.; Vasavada, A. R.; Veverka, J.; Wagner, R.; West, R. (2005) Cassini Imaging Science: Initial Results on Saturn's Rings and Small Satellites; Science, 307, 5713, 1226-1236

Porco, C. C.; Thomas, P. C.; Weiss, J. W.; Richardson, D. C.(2007) Saturn's Small Inner Satellites: Clues to Their Origins; Science 318, 1602

Porco, C. C.; Weiss, J. W.; Richardson, D. C.; Dones, L.; Quinn, T.; Throop, H. (2008) Simulations of the Dynamical and Light-Scattering Behavior of Saturn's Rings and the Derivation of Ring Particle and Disk Properties; A.J. 136, 2172-2200

Porco, C. C.; Weiss, J. W.; Richardson, D. C.; Dones, L.; Quinn, T.; Throop, H. (2008) Simulations of the Dynamical and Light-Scattering Behavior of Saturn's Rings and the Derivation of Ring Particle and Disk Properties; AJ 136, 2172-2200

Poulet, F.; Sicardy, B. (2001) Dynamical evolution of the Prometheus-Pandora system; MNRAS 322, 343-355.

Poulet, F.; Cuzzi, J. N. (2002) The Composition of Saturn's Rings; Icarus 160, 350-358.

Poulet, F.; Cruikshank, D. P.; Cuzzi, J. N.; Roush, T. L.; French, R. G. (2003) Compositions of Saturn's rings A, B, and C from high resolution near-infrared spectroscopic observations; Astron. Astrophys 412, 305-316

Reffet, E., Verdier, M., and Ferrari, C. 2015. Thickness of Saturn's B ring as derived from seasonal temperature variations measured by Cassini CIRS. *Icarus*, **254**, 276–286.

Rein, H.; Papaloizou, J. C. B. (2010) Stochastic orbital migration of small bodies in Saturn's rings; Astron. Astrophys 524, id.A22, 13 pp.

Robbins, S. J., Stewart, G. R., Lewis, M. C., Colwell, J. E., and Sremcević, M. (2010) Estimating the masses of Saturn's A and B rings from high-optical depth N-body simulations and stellar occultations. Icarus, 206, 431–445.

Salo, H.; French, R.G. (2010) The opposition and tilt effects of Saturn's rings from HST observations; Icarus 210, 785-816.

Schmidt, J.; Ohtsuki, K.; Rappaport, N.; Salo, H.; Spahn, F. (2009) Dynamics of Saturn's Dense Rings; in Saturn from Cassini-Huygens, by Dougherty, M. K.; Esposito, L. W.; Krimigis, S. M., ISBN 978-1-4020-9216-9. Springer Science+Business Media B.V., 2009, p. 213

Schmidt, J.; Colwell, J. E.; Lehmann, M.; Marouf, E. A.; Salo, H.; Spahn, F.; Tiscareno, M. S. (2016) On the Linear Damping Relation for Density Waves in Saturn's Rings; ApJ 824, Issue 1, article id. 33

Schmidt, J.; Tiscareno, M. S. (2013) Ejecta clouds from meteoroid impacts on Saturn's rings: Constraints on the orbital elements and size of the projectiles; AGU Fall Meeting 2013, abstract id.P23D-1820

Schaffer, L.; Burns, J. A. (1987) The dynamics of weakly charged dust - Motion through Jupiter's gravitational and magnetic fields; JGR 92, 2264-2280

Seiler, M.; Sremčević, M.; Seiß, M.; Hoffmann, H.; Spahn, F. (2017) A Librational Model for the Propeller Blériot in the Saturnian Ring System; ApJL 840, Issue 2, article id. L16

Shimizu, M. (1982) Strong interaction between the ring system and the ionosphere of Saturn; Moon and the Planets, 22, p. 521, 522.

Showalter, Mark R. (1991) Visual detection of 1981S13, Saturn's eighteenth satellite, and its role in the Encke gap; Nature 351, 709-713.

Showalter, M. R.; Nicholson, P. D. (1990) Saturn's rings through a microscope - Particle size constraints from the Voyager PPS scan; Icarus 87, 285-306.

Shu, F. H. (1984) Waves in planetary rings; in "Planetary Rings" (A85-34401 15-88). University of Arizona Press, 1984, p. 513-561.

Smith, B. A.; Soderblom, L.; Batson, R. M.; Bridges, P. M.; Inge, J. L.; Masursky, H.; Shoemaker, E.; Beebe, R. F.; Boyce, J.; Briggs, G.; Bunker, A.; Collins, S. A.; Hansen, C.; Johnson, T. V.; Mitchell, J. L.; Terrile, R. J.; Cook, A. F.; Cuzzi, J. N.; Pollack, J. B.; Danielson, G. E.; Ingersoll, A. P.; Davies, M. E.; Hunt, G. E.; Morrison, D.; Owen, T.; Sagan, C.; Veverka, J.; Strom, R.; Suomi, V. E. (1982) A new look at the Saturn system - The Voyager 2 images; Science 215, 504-537.

Spahn, F.; Scholl, H.; Hertzsch, J.-M. (1994) Structures in planetary rings caused by embedded moonlets; Icarus 111, 514-535

Spahn, F., H. Hoffmann, H. Rein, M. Seiss, M. Sremcevic, and M. Tiscareno (2018) Moonlets in Dense Planetary Rings; in "Planetary Rings": M. Tiscareno and C. Murray, eds. (Cambridge) p. 157-197

Spilker, L. J., Pilorz, S. H., Edgington, S. G., *et al.* 2005. Cassini CIRS observations of a roll-off in Saturn ring spectra at submillimeter wavelengths. *Earth Moon Planets*, 96, 149–163.

Spilker, L. J., C. Ferrari, N. Altobelli, S. Pilorz, and R. Morishima (2018) Thermal Properties of Rings and Ring Particles; a chapter in ``Planetary Rings'': M. Tiscareno and C. Murray, eds. (Cambridge) p. 397-431

Spitale, J. N.; Hahn, J. M. (2016) The shape of Saturn's Huygens ringlet viewed by Cassini ISS; Icarus 279, 141-154.

Spitale, J. N. (2017) Saturn's Misbegotten Moonlets; AAS/DDA meeting #48, id.400.04

Spitale, J. N.; Jacobson, R. A.; Porco, C. C.; Owen, W. M., Jr. (2006) The Orbits of Saturn's Small Satellites Derived from Combined Historic and Cassini Imaging Observations; Astron. J. 132, 692-710.

Spitale, J. N.; Porco, C. C. (2009) Time Variability in the Outer Edge of Saturn's A-Ring Revealed by Cassini Imaging; Astron. J. 138, 1520-1528

Spitale, J. N.; Porco, C. C. (2010) Detection of Free Unstable Modes and Massive Bodies in Saturn's Outer B Ring; AJ 140, 1747-1757

Sremcevic, M.; Krivov, A. V.; Krüger, H.; Spahn, F. (2005) Impact-generated dust clouds around planetary satellites: model versus Galileo data; Plan. Sp. Sci 53, 625-641.

Sremčević, M.; Schmidt, J.; Salo, H.; Seisz, M.; Spahn, F.; Albers, N. (2007) A belt of moonlets in Saturn's A ring; Nature 449, 1019-1021

Sremcevic, M.; Stewart, G. R.; Albers, N.; Esposito, L. W. (2012) Discovery Of B Ring Propellers In Cassini UVIS And ISS; AAS/DPS meeting #44, id.513.06

Sremcevic, M.; Stewart, G. R.; Albers, N.; Esposito, L. W. (2013) Propellers in Saturn's rings; AGU Fall Meeting 2013, abstract id.P21E-07

Sremcevic, M.; Stewart, G. R.; Albers, N.; Esposito, L. W. (2014a) Propellers in Saturn's rings; EPSC Abstracts, Vol. 9, id. EPSC2014-633

Sremcevic, M.; Stewart, G. R.; Albers, N.; Esposito, L.W. (2014b) Propellers in Saturn A and B rings; AAS/DPS meeting #46, id.417.01

Tajeddine, R.; Lainey, V.; Cooper, N. J.; Murray, C. D. (2013) Cassini ISS astrometry of the Saturnian satellites: Tethys, Dione, Rhea, Iapetus, and Phoebe 2004-2012; A&A 575, id.A73, 6 pp.

Tajeddine, R.; Nicholson, P. D.; Longaretti, P.-Y.; El Moutamid, M.; Burns, J. A. (2017a) What Confines the Rings of Saturn? ApJS 232, Issue 2, article id. 28, 17 pp.

Tajeddine, R.; Nicholson, P. D.; Tiscareno, M. S.; Hedman, M. M.; Burns, J.A.; El Moutamid, M. (2017b) Dynamical phenomena at the inner edge of the Keeler gap; Icarus 289, 80-93.

Tamayo, D.; Hedman, M. M.; Burns, J. A. (2014) First observations of the Phoebe ring in optical light; Icarus 233, p. 1-8.

Tamayo, D.; Markham, S. R.; Hedman, M. M.; Burns, J. A.; Hamilton, D.P. (2016) Radial profiles of the Phoebe ring: A vast debris disk around Saturn; Icarus 275, 117-131.

Thomson, F. S.; Marouf, E. A.; Tyler, G. L.; French, R. G.; Rappoport, N. J. (2007) Periodic microstructure in Saturn's rings A and B; GRL 34, Issue 24, CiteID L24203

Tiscareno, M. S.; Burns, J. A.; Hedman, M.M.; Porco, C. C.; Weiss, J. W.; Dones, L.; Richardson, D. C.; Murray, C. D. (2006) 100-metre-diameter moonlets in Saturn's A ring from observations of ‘propeller’ structures; Nature 440, Issue 7084, 648-650

Tiscareno, M. S.; Burns, J. A.; Nicholson, P. D.; Hedman, M. M.; Porco, C. C. (2007) Cassini imaging of Saturn's rings. II. A wavelet technique for analysis of density waves and other radial structure in the rings; Icarus 189, 14-34.

Tiscareno, M.S.; Burns, J.A.; Hedman, M. M.; Porco, C. C. (2008) The Population of Propellers in Saturn's A Ring; Astron. J. 135, 1083-1091

Tiscareno, M. S.; Burns, J. A.; Sremcevic, M.; Beurle, K.; Hedman, M. M.; Cooper, N. J.; Milano, A. J.; Evans, M. W.; Porco, C. C.; Spitale, J. N.; Weiss, J.W. (2010) Physical Characteristics and Non-Keplerian Orbital Motion of "Propeller" Moons Embedded in Saturn's Rings; ApJ 718, L92-L96

Tiscareno, M. S.; Hedman, M.M.; Burns, J. A.; Weiss, J.W.; Porco, C. C. (2013a) Probing the inner boundaries of Saturn's A ring with the Iapetus -1:0 nodal bending wave; Icarus 224, 201-208.

Tiscareno, M. S.; Mitchell, C. J.; Murray, C. D.; Di Nino, D.; Hedman, M. M.; Schmidt, J.; Burns, J. A.; Cuzzi, J.N.; Porco, C. C.; Beurle, K.; Evans, M. W. (2013b) Observations of Ejecta Clouds Produced by Impacts onto Saturn's Rings; Science 340, Issue 6131, 460-464

Tiscareno, Matthew S. (2013) A modified "Type I migration" model for propeller moons in Saturn's rings; Plan. & Sp. Sci 77, 36-142.

Tiscareno, M. S.; Harris, B. E. (2018) Mapping spiral waves and other radial features in Saturn's rings; eprint arXiv:1708.03702; Submitted to Icarus

Tiscareno, M.S.; Mitchell, C. J.; Murray, C. D.; Di Nino, D.; Hedman, Ma.M.; Schmidt, J.; Burns, J. A.; Cuzzi, J. N.; Porco, C.C.; Beurle, K.; Evans, M. W. (2013); Observations of Ejecta Clouds Produced by Impacts onto Saturn's Rings; Science, 340, 6131, 460-464

Tseng, W.-L.; Ip, W.-H.; Johnson, R. E.; Cassidy, T. A.; Elrod, M. K. (2010) The structure and time variability of the ring atmosphere and ionosphere; Icarus, 206, 382-389.

Tseng, W.-L.; Johnson, R. E.; Elrod, M. K. (2013) Modeling the seasonal variability of the plasma environment in Saturn's magnetosphere between main rings and Mimas; Plan. Sp. Sci. 77, 126-135

Vahidinia, S.; Cuzzi, J.N.; Hedman, M.; Draine, B.; Clark, R. N.; Roush, T.; Filacchione, G.; Nicholson, P. D.; Brown, R. H.; Buratti, B.; Sotin, C.(2011) Saturn's F ring grains: Aggregates made of crystalline water ice; Icarus 215, Issue 2, p. 682-694. [Erratum: 2012Icar..218..736V]

van Allen, J. A. (1982) Findings on rings and inner satellites of Saturn of Pioneer 11; Icarus 51, 509-527

Verbiscer, A. J.; Skrutskie, M. F.; Hamilton, D.P. (2009) Saturn's largest ring; Nature 461, 1098-1100

Waite et al 2018 Science

Weiss, J. W.; Porco, C. C.; Tiscareno, M.S. (2009) Ring Edge Waves and the Masses of Nearby Satellites; AJ 138, 272-286

Ye, S_Y., Gurnett D.A. and Kurth, W.S., In-situ measurements of Saturn's dusty rings based on dust impact signals detected by Cassini RPWS Icarus 279: 51-61

Zebker, H. A.; Marouf, E. A.; Tyler, G. L. (1985) Saturn's rings - Particle size distributions for thin layer model; Icarus 64, 531-548.

Zhang, Z.; Hayes, A. G.; Janssen, M. A.; Nicholson, P. D.; Cuzzi, J. N.; de Pater, I.; Dunn, D. E.; Estrada, P. R.; Hedman, M. M. (2017a) Cassini microwave observations provide clues to the origin of Saturn's C ring; Icarus, 281, 297-321.

Zhang, Z.; Hayes, A. G.; Janssen, M. A.; Nicholson, P. D.; Cuzzi, J. N.; de Pater, I.; Dunn, D. E. (2017b) Exposure age of Saturn's A and B rings, and the Cassini Division as suggested by their non-icy material content; Icarus 294, 14-42.